Regulation of Murine Inflammatory Bowel Disease by $CD25^+$ and $CD25^-$ $CD4^+$ Glucocorticoid-Induced TNF Receptor Family-Related $Gene^+$ Regulatory T Cells[1]

Koji Uraushihara,[2†] Takanori Kanai,[2,3†] Kwibeom Ko,[*] Teruji Totsuka,[†] Shin Makita,[†] Ryoichi Iiyama,[†] Tetsuya Nakamura,[†] and Mamoru Watanabe[†]

$CD4^+CD25^+$ regulatory T cells in normal animals are engaged in the maintenance of immunological self-tolerance and prevention of autoimmune disease. However, accumulating evidence suggests that a fraction of the peripheral $CD4^+CD25^-$ T cell population also possesses regulatory activity in vivo. Recently, it has been shown glucocorticoid-induced TNFR family-related gene (GITR) is predominantly expressed on $CD4^+CD25^+$ regulatory T cells. In this study, we show evidence that $CD4^+GITR^+$ T cells, regardless of the CD25 expression, regulate the mucosal immune responses and intestinal inflammation. SCID mice restored with the $CD4^+GITR^-$ T cell population developed wasting disease and severe chronic colitis. Cotransfer of $CD4^+GITR^+$ population prevented the development of $CD4^+CD45RB^{high}$ T cell-transferred colitis. Administration of anti-GITR mAb-induced chronic colitis in mice restored both $CD45RB^{high}$ and $CD45RB^{low}$ $CD4^+$ T cells. Interestingly, both $CD4^+CD25^+$ and $CD4^+CD25^-$ $GITR^+$ T cells prevented wasting disease and colitis. Furthermore, in vitro studies revealed that $CD4^+CD25^-GITR^+$ T cells as well as $CD4^+CD25^+GITR^+$ T cells expressed CTLA-4 intracellularly, showed anergic, suppressed T cell proliferation, and produced IL-10 and TGF-β. These data suggest that GITR can be used as a specific marker for regulatory T cells controlling mucosal inflammation and also as a target for treatment of inflammatory bowel disease. *The Journal of Immunology,* **2003, 171: 708–716.**

The gastrointestinal tract is home to the largest number of leukocytes in the body as well as being the site in which these cells encounter abundant exogenous stimuli. Despite this potential immune stimulus, it is well known that immune responses in the intestine remain in a state of controlled inflammation (1). Regulation of the immune response here is a balance between the need to mount protective immunity toward pathogens while not activating damaging inflammatory responses to the plethora of harmless Ags present, including those derived from resident bacteria (2). To maintain the intestinal homeostasis, including immunological tolerance, functionally distinct subsets have been clearly defined in T cells (3, 4). Among these subsets, regulatory T cell subset down-regulates immune responses for both foreign and self Ags and effectively participates in the suppression of autoimmune disorders (5–7). The importance of an intact immune system for the intestinal homeostasis is revealed by the fact that a number of immune manipulations, including deletion of cytokine genes and alterations in T cell subsets, lead to the development of an inflammatory bowel disease (IBD)[4] (8–10). Evidence emerging from these studies suggests that pathogenic responses in the intestine are derived by resident bacteria and controlled by a functionally specialized population of regulatory T cells in the gut-associated lymphoid tissue (11).

A variety of cells that display regulatory function in vitro or in vivo have been described. These can be subdivided into different subsets based on the expression of cell surface markers, production of cytokines, and mechanisms of action. Recent studies focused on CD25 as the best marker for regulatory $CD4^+$ T cells in mice and humans (12–14). $CD4^+CD25^+$ T cells, which constitute ~10% of peripheral murine $CD4^+$ T cells, express little CD45RB, and a significant proportion expresses CTLA-4 (15–18). They show a partially anergic phenotype, in that they proliferate poorly upon TCR stimulation in vitro and their growth is dependent on exogenous IL-2.

However, increasing evidence suggests that the peripheral $CD4^+CD25^-$ T cell population also possesses some regulatory activity (19–24), although specific markers for $CD4^+CD25^-$ regulatory T cells remain unclear. Stephens and Mason (23) have described a population of $CD4^+CD25^-$ T cells that can prevent autoimmunity in thymectomy/irradiation model in rat, but only if recent $CD25^-$ thymic emigrants have been deleted from the population. Similarly, $CD4^+CD25^-$ T cells appear to be responsible for the resistance of mice expressing a transgenic TCR specific for myelin basic protein to the spontaneous development of autoimmune encephalomyelitis (20). In fact, $CD4^+CD25^+$ T cell population is heterogeneous, and although a relatively high proportion of these cells may be regulatory T cells, but it is not likely to be

*Department of Experimental Pathology, Institute for Frontier Medical Sciences, Kyoto University, Kyoto, Japan; and †Department of Gastroenterology and Hepatology, Graduate School, Tokyo Medical and Dental University, Tokyo, Japan

Received for publication February 19, 2003. Accepted for publication May 7, 2003.

The costs of publication of this article were defrayed in part by the payment of page charges. This article must therefore be hereby marked *advertisement* in accordance with 18 U.S.C. Section 1734 solely to indicate this fact.

[1] This work was supported in part by grants-in-aid from the Japanese Ministry of Education, Culture, and Science; the Japanese Ministry of Health and Welfare; Okawa Intractable Disease Research Foundation; and Japan Health Sciences Foundation.

[2] K.U. and T.K. contributed equally to this work.

[3] Address correspondence and reprint requests to Dr. Takanori Kanai, Department of Gastroenterology and Hepatology, Graduate School, Tokyo Medical and Dental University, 1-5-45 Yushima, Bunkyo-ku, Tokyo 113-8519, Japan. E-mail address: taka.gast@tmd.ac.jp

[4] Abbreviations used in this paper: IBD, inflammatory bowel disease; GITR, glucocorticoid-induced TNFR family-related gene; HA, hemagglutinin; HPF, high power field; IEL, intraepithelial cell; LP, lamina propria; LPMC, lamina propria mononuclear cell.

0022-1767/03/$02.00

true that the entire population is regulatory or that all regulatory T cells express CD25.

Very recently, it has been demonstrated that glucocorticoid-induced TNFR family-related gene (GITR), a member of the TNF-nerve growth factor receptor gene superfamily, is predominantly expressed on $CD4^+CD25^+$ T cells and on $CD4^+CD25^+CD8^-$ thymocytes in normal naive mice (25). In addition, removal of GITR-expressing T cells or administration of a mAb to GITR produced organ-specific autoimmune disease in otherwise normal mice (25).

In the present study, we conducted a series of experiments focusing on GITR as a regulatory T cell marker for intestinal mucosal regulatory T cell to investigate the characteristics of $CD4^+CD25^-$ regulatory T cells, and to understand how the mucosal immune system is controlled by GITR-associated regulatory T cells.

Materials and Methods

Animals

Female BALB/c, C.B-17 SCID, and C57BL/6 mice were purchased from Japan Clear (Tokyo, Japan). Mice were maintained under specific pathogen-free conditions in the Animal Care Facility of Tokyo Medical and Dental University. Mice were used at 7–12 wk of age. All experiments were approved by the regional animal study committees.

Antibodies

The following mAbs and reagents were purchased from BD PharMingen (San Diego, CA), except anti-mouse GITR mAb (DTA-1, rat IgG2a), and used for purification of cell populations and flow cytometry analysis: RM4-5, PE-conjugated anti-mouse CD4 (rat IgG2a); 7D4, FITC-conjugated anti-mouse CD25 (rat IgM); PC61, PE-conjugated anti-mouse CD25 (rat IgG1); DTA-1, biotinylated anti-GITR (25); 9H10, PE-conjugated anti-CTLA-4 (hamster IgG); M290, PE-conjugated anti-mouse CD103 (α_E integrin) (rat IgG2a); PK136, PE-conjugated anti-mouse NK1.1 (mouse IgG2a); DX5, FITC-conjugated anti-mouse pan-NK cells (rat IgM); H28-710, FITC-conjugated anti-mouse TCR α-chain (hamster IgG); GL4, FITC-conjugated anti-mouse TCR $\gamma\delta$-chains (hamster IgG); isotype control Abs, biotin-conjugated rat IgG2, FITC-conjugated rat IgM, PE-conjugated rat IgG2a, and PE-conjugated mouse IgG2a; PE-conjugated streptavidin; CyChrome-conjugated streptavidin.

Purification of T cell subsets

$CD4^+$ T cells were isolated from spleen cells from BALB/c mice using the anti-CD4 (L3T4) MACS system (Miltenyi Biotec, Auburn, CA), according to the manufacturer's instruction. Enriched $CD4^+$ T cells (96–97% pure, as estimated by a FACSCalibur (BD Biosciences, Sunnyvale, CA)) were then labeled with PE-conjugated anti-mouse CD4 (RM4-5), FITC-conjugated anti-CD45RB (16A), FITC-conjugated anti-CD25 (7D4), biotinylated anti-GITR mAb (DTA-1), and streptavidin PE. Subpopulations of $CD4^+$ cells were generated by two-color sorting on a FACSVantage (BD Biosciences). All populations were >98.0% pure on reanalysis.

In vivo experimental design

We performed a series of in vivo experiments below to investigate the role of $CD4^+GITR^+$ T cells on the regulation of murine chronic colitis. Experiment 1: To assess regulatory T cell activity in $CD4^+GITR^+$ T cells, we used the classical SCID-transfer colitis model (26). C.B-17 SCID mice were injected i.p. with one or two subpopulations of sorted $CD4^+$ T cell in PBS: 1) $CD4^+CD45RB^{high}$ alone (3×10^5 per body, as a positive control); 2) $CD4^+CD45RB^{high}$ + $CD4^+CD45RB^{low}$ (each 3×10^5 per body, as a negative control); 3) $CD4^+CD45RB^{high}$ (3×10^5 per body) + $CD4^+GITR^+$ (1×10^5 per body); or 4) $CD4^+GITR^-$ alone (3×10^5 per body). Mice were sacrificed at 4 wk after T cell transfer, because percentage of decrease of original body weight in one of experimental group reached 20%. Experiment 2: To assess functional role of GITR, we used purified anti-murine GITR mAb (rat IgG2a, DTA-1). C.B-17 SCID mice were injected i.p. with $CD4^+CD45RB^{high}$ + $CD4^+CD45RB^{low}$ T cells (each 3×10^5 per body, as a negative control), and also were given 1 mg control rat IgG or anti-GITR mAb by i.p. injection weekly from the day of T cell transfer over a period of 6 wk. As a positive control, C.B-17 SCID mice were injected i.p. with $CD4^+CD45RB^{high}$ T cells alone (3×10^5 per body). Experiment 3: To address the possibility that $CD4^+CD25^-$ T cells in $CD4^+GITR^+$ T cell population function as regulatory T cells, we divided $CD4^+GITR^+$ T cells into $CD4^+CD25^-GITR^+$ and $CD4^+CD25^+GITR^+$ cells. C.B-17 SCID mice were then injected i.p. with one or two subpopulations of sorted $CD4^+$ T cell in PBS: 1) $CD4^+CD45RB^{high}$ + $CD4^+CD45RB^{low}$ (each 3×10^5 per body, as a negative control); 2) $CD4^+CD45RB^{high}$ alone (3×10^5 per body, as a postive control); 3) $CD4^+CD45RB^{high}$ (3×10^5 per body) + $CD4^+CD25^+GITR^+$ cells (1×10^5 per body); or 4) $CD4^+CD45RB^{high}$ (3×10^5 per body) + $CD4^+CD25^-GITR^+$ cells (1×10^5 per body). Mice were sacrificed and analyzed 7 wk after T cell transfer.

Disease monitoring and clinical scoring

The recipient SCID mice after T cell transfer were weighed initially, then three times per week thereafter. They were observed for clinical signs of illness: hunched over appearance, piloerection of the coat, diarrhea, and blood in the stool. Mice were sacrificed and assessed for a clinical score that is the sum of four parameters, as follows: hunching and wasting, 0 or 1; colon thickening, 0–3 (0, no colon thickening; 1, mild thickening; 2, moderate thickening; 3, extensive thickening); and stool consistency, 0–3 (0, normal beaded stool; 1, soft stool; 2, diarrhea; and an additional point was added if gross blood was noted) (27).

Histological examination

Tissue samples were fixed in PBS containing 6% neutral-buffered Formalin. Paraffin-embedded sections (5 μm) were stained with H&E. Three tissue samples from the proximal, middle, and distal parts of the colon were prepared. The sections were analyzed without prior knowledge of the type of T cell reconstitution or treatment. The area most affected was graded by the number and severity of lesions. The mean degree of inflammation in the colon was calculated using a modification of a previously described scoring system (28), as follows: mucosa damage, 0; normal, 1; 3–10 intraepithelial cells (IEL)/high power field (HPF) and focal damage, 2; >10 IEL/HPF and rare crypt abscesses, 3; >10 IEL/HPF, multiple crypt abscesses and erosion ulceration, submucosa damage, 0; normal or widely scattered leukocytes, 1; focal aggregates of leukocytes, 2; diffuse leukocyte infiltration with expansion of submucosa, 3; diffuse leukocyte infiltration, muscularis damage, 0; normal or widely scattered leukocytes, 1; widely scattered leukocyte aggregates between muscle layers, 2; leukocyte infiltration with focal effacement of the muscularis, 3; extensive leukocyte infiltration with transmural effacement of the muscularis.

Preparation of mucosal lamina propria mononuclear cells

Colonic lamina propria mononuclear cells (LPMCs) were isolated using a method, as described previously (29). In brief, the entire length of intestine was opened longitudinally, washed with PBS, and cut into small (~5-mm) pieces. To remove epithelium including IEL, the dissected mucosa was incubated twice with Ca^{2+} Mg^{2+}-free HBSS containing 1 mM DTT (Sigma-Aldrich, St. Louis, MO) for 30 min, and then serially incubated twice in medium containing 0.75 mM EDTA (Sigma-Aldrich) for 60 min at 37°C under gentle shaking. The supernatants from these incubations, which included the epithelium and IELs, were deserted, and the residual fragments were pooled and treated with 2 mg/ml collagenase A (Worthington Biomedical, Freehold, NJ) and 0.01% DNase (Worthington) in 5% CO_2 humidified air at 37°C for 2 h. The cells were then pelleted twice through a 40% isotonic Percoll solution, after which they were further purified by Ficoll-Hypaque (Pharmacia, Uppsala, Sweden) density-gradient centrifugation (40/75%). Enriched lamina propria (LP) $CD4^+$ T cells were obtained by positive selection using an anti-CD4 (L3T4) MACS magnetic separation system. The resultant cells when analyzed by FACSCalibur contained >96% $CD4^+$ cells.

Flow cytometry

To detect the surface expression of a variety of molecules, isolated splenocytes or LPMCs were preincubated with an FcγR-blocking mAb (CD16/32; 2.4G2; BD PharMingen) for 20 min, followed by incubation with specific FITC-, PE-, or biotin-labeled Abs for 30 min on ice. The mAbs used were anti-CD4 mAb, anti-CD25 mAb, anti-CD45RB, anti-GITR, anti-TCRα, anti-TCR$\gamma\delta$, anti-NK1.1, and anti-pan NK cell (DX5) mAbs. Biotinylated Abs were detected with PE or CyChrome streptavidin. Standard two- or three-color flow cytometric analyses were obtained using the FACSCalibur utilizing CellQuest software. Background fluorescence was assessed by staining with control isotype-matched mAbs.

Cytokine ELISA

To measure cytokine production, 1×10^5 LP $CD4^+$ T cells were cultured in 200 μl culture medium at 37°C in a humidified atmosphere containing

5% CO_2 in 96-well plates (Costar, Cambridge, MA) precoated with 5 μg/ml hamster anti-mouse CD3ε mAb (145-2C11; BD PharMingen) and hamster 2 μg/ml anti-mouse CD28 mAb (37.51; BD PharMingen) in PBS overnight at 4°C. Culture supernatants were removed after 48 h and assayed for cytokine production. Cytokine concentrations were determined by specific ELISA per manufacturer's recommendation (R&D Systems, Minneapolis, MN).

In vitro regulatory T cell function in $CD4^+CD25^-GITR^+$ T cells

Spleen cells from BALB/c mice were separated into unfractioned whole $CD4^+$ T cells, $CD4^+CD25^+GITR^+$ T cells, and $CD4^+CD25^-GITR^+$ T cells using the anti-CD4 (L3T4) MACS magnetic separation system and FACSVantage, as described above. Cells (5×10^4) and *x*-irradiated (20 Gy) BALB/c $CD4^-$ cells (2×10^5), as APCs, were cultured for 72 h in round-bottom 96-well plates in RPMI supplemented with 10% FCS, 100 IU/ml penicillin, 100 μg/ml streptomycin, 2 mM glutamine, 1 mM sodium pyruvate, and 50 μM 2-ME. Cells were stimulated with Con A (5 μg/ml) in the presence or absence of human rIL-2 (100 U/ml). In coculture experiments, 2-fold numbers of $CD4^+CD25^+GITR^+$ cells, $CD4^+CD25^-GITR^+$ cells, or whole $CD4^+$ cells (as a control) (1×10^5) were added into wells with the fixed dose of whole $CD4^+$ cells (5×10^4) and *x*-irradiated (20 Gy) $CD4^-$ cells (2×10^5), as APCs. Incorporation of [^{3}H]thymidine (1 μCi/well) by proliferating cells was measured during the last 9 h of culture. For cytokine assays, purified $CD4^+CD25^+GITR^+$, $CD4^+CD25^-GITR^+$ T cells, or whole $CD4^+$ cells were cultured in complete medium consisting of RPMI 1640 (or serum-free medium (Nutridoma SP; Roche Molecular, Mannheim, Germany) in the case of TGF-β) in flat-bottom 96-well plates (200 μl) at 2×10^5 cells/well and stimulated with 10 μg/ml plate-bound anti-CD3 mAb plus soluble anti-CD28 mAb (5 μg/ml). Supernatants were collected after 24 h for IL-2; 48 h for IL-4, IL-10, and IFN-γ; and 72 h for TGF-β. Cytokines secreted into culture fluid were assayed by ELISA kits. Levels of TGF-β in acidified supernatants were determined by TGF-β1 Emax Immunoassay Kit (Promega, Madison, WI), according to the manufacturer's instructions. Other cytokines were measured by specific ELISA per manufacturer's recommendation (R&D Systems). For the analysis of CTLA-4 expression, $CD4^+$ cells were sorted by FITC-conjugated anti-CD25 and biotinylated anti-GITR, followed by CyChrome-conjugated streptavidin. After sorting cells using a FACSVantage, cells were stained with PE-conjugated anti-CTLA-4 mAb. Before staining with anti-CTLA-4 mAb, the cells were fixed and permeabilized with Cytofix/Cytoperm (BD PharMingen) at 4°C for 30 min. Staining and washing were performed in Perm/Wash Buffer (BD PharMingen), and cells were washed once in PBS before analysis.

Statistical analysis

The results were expressed as the mean ± SD. Groups of data were compared by Mann-Whitney *U* test. Differences were considered to be statistically significant when $p < 0.05$.

Results

Murine splenic $CD4^+$ T cells contain both $CD4^+CD25^+GITR^+$ and $CD4^+CD25^-GITR^+$ T cells

Efforts to delineate regulatory T cell population have revealed that $CD4^+CD25^+$ T cell population in mice and humans retains regulatory T cell function (12, 30–33). However, accumulating evidence has shown that $CD4^+CD25^-$ T cell population also possesses regulatory activity (19–24), although specific markers for $CD4^+CD25^-$ regulatory T cells remain unclear. Recently, Shimizu et al. (25) have reported that GITR, a member of TNF/TNFR family, is a functional specific marker as regulatory T cells. In this study, we first postulated that both $CD4^+CD25^+$ and $CD4^+CD25^-$ regulatory T cells express GITR. Thus, we assessed the correlation among the expression of GITR, CD25, and CD45RB on freshly isolated splenocytes. First, GITR was mainly expressed on $CD4^+$ T cells (Fig. 1*A*, *lower left panel*). As expected, $CD25^+$ cells expressed GITR (Fig. 1*A*, *upper right panel*). Interestingly, GITR-expressing cells also existed to some degree in $CD25^-$ subpopulation (Fig. 1*A*, *upper right panel*). Importantly, GITR was exclusively expressed on $CD45RB^{low}$ cells (Fig. 1*A*, *lower right panel*). Three-color flow cytometric analysis revealed that $GITR^+$ cells in MACS-sorted $CD4^+$ T cells contain both

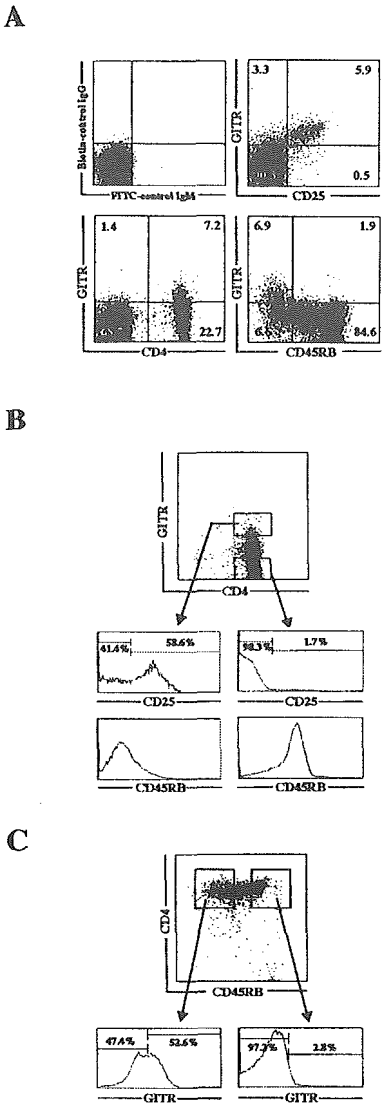

FIGURE 1. Murine splenic $CD4^+$ T cells contain both $CD4^+CD25^+GITR^+$ and $CD4^+CD25^-GITR^+$ T cells. *A*, GITR expression on murine splenocytes. Isolated splenocytes were analyzed for cell surface expression of GITR, CD25, and CD45RB. As isotype controls, biotin-conjugated rat IgG2a and FITC-conjugated rat IgM were used for their staining with biotin-conjugated anti-GITR and GITC-conjugated anti-CD25, respectively. *B*, CD25 and CD45RB expression by $CD4^+GITR^+$ T cells. Freshly isolated splenic $CD4^+$ T cells by anti-CD4-MACS beads were stained with anti-CD4, anti-GITR, anti-CD25, and anti-CD45RB mAbs. *C*, GITR expression by $CD4^+CD45RB^{high}$ and $CD4^+CD45RB^{low}$ T cells. MACS-sorted $CD4^+$ T cells were stained with anti-CD4, anti-CD45RB, and anti-GITR mAbs.

$CD25^+$ (60.3 ± 6.4%) and $CD25^-$ (39.3 ± 4.9%) fractions, although $CD4^+GITR^-$ T cells were mostly $CD25^-$ (Fig. 1*B*). In addition, this analysis confirmed that $CD4^+GITR^+$ T cells are mostly $CD45RB^{low}$ (Fig. 1*B*). These data indicate that GITR expression is a possible clue of the correlation between $CD4^+CD25^+$ (12) and $CD4^+CD45RB^{low}$ (8) regulatory T cells. Finally, we confirmed that approximately one-half of $CD4^+CD45RB^{low}$ T cell fraction was $GITR^+$ T cells, although $CD4^+CD45RB^{high}$ T cells were mostly $GITR^-$ (Fig. 1*C*).

$CD4^+GITR^+$ T cells inhibited the development of the classical $CD4^+CD45RB^{high}$-transferred colitis

To analyze the functional role of $CD4^+GITR^+$ or $CD4^+GITR^-$ subset in vivo, we first tested the regulatory activity of $CD4^+$

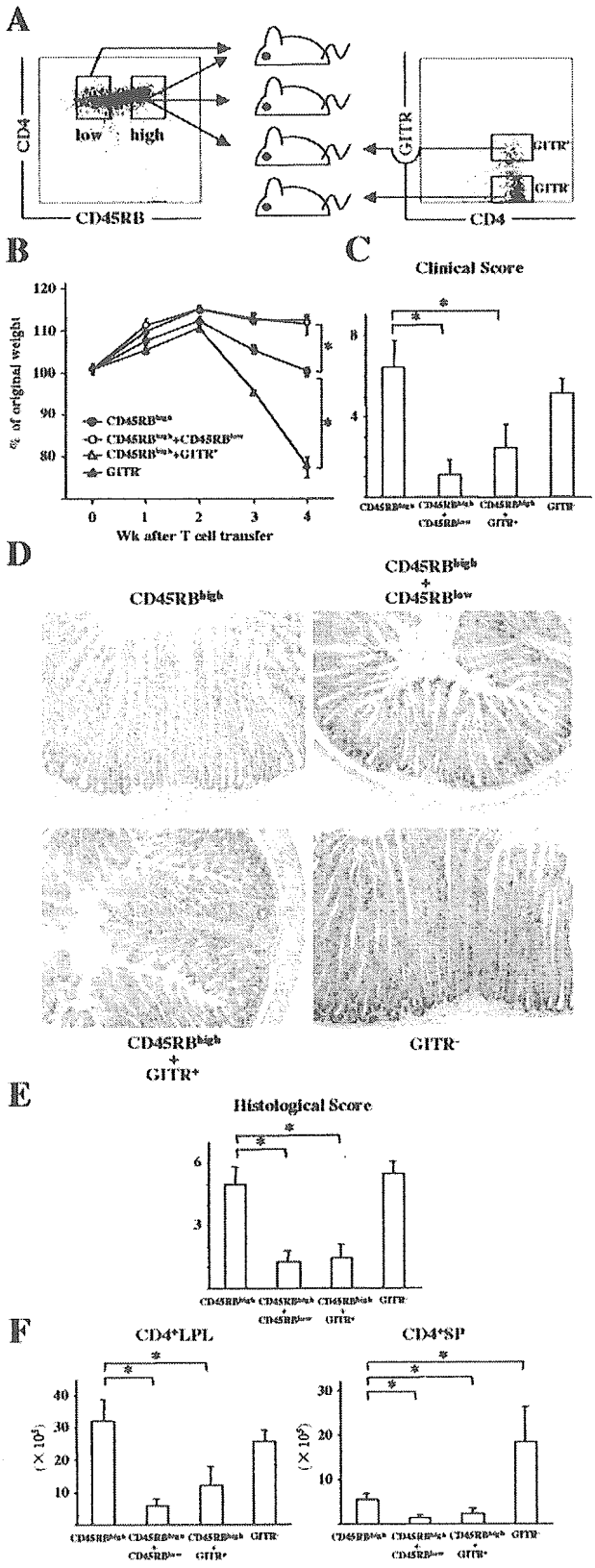

FIGURE 2. $CD4^+GITR^+$ T cells inhibited the development of the classical $CD4^+CD45RB^{high}$-transferred colitis. *A*, C.B-17 SCID mice were injected i.p. with: 1) $CD4^+CD45RB^{high}$ T cells alone (3×10^5 per body, as a positive control); 2) $CD4^+CD45RB^{high}$ + $CD4^+CD45RB^{low}$ T cells (each 3×10^5 per body, as a negative control); 3) $CD4^+CD45RB^{high}$ (3×10^5 per body) + $CD4^+GITR^+$ T cells (1×10^5 per body); or 4) $CD4^+GITR^-$ T cells alone (3×10^5 per body) to create four different groups (seven animals per each group). *B*, $CD4^+GITR^+$ T cells inhibited a wasting disease. Recipient SCID mice were weighed on the day of T cell transfer and three times per week thereafter; ●, $CD4^+CD45RB^{high}$; □, $CD4^+CD45RB^{high}$ + $CD4^+CD45RB^{low}$; △, $CD4^+CD45RB^{high}$ + $CD4^+GITR^+$; and ▲, $CD4^+GITR^-$. Statistical analysis was performed to compare the slopes of the weight change between the groups of mice that received $CD4^+CD45RB^{high}$ + $CD4^+CD45RB^{low}$ or $CD4^+CD45RB^{high}$ + $CD4^+GITR^+$ T cells with mice that received $CD4^+CD45RB^{high}$ T cells. *, $p < 0.05$. *C*, $CD4^+GITR^+$ T cells inhibited a chronic colitis. Clinical scores were determined at 4 wk after transfer, as described in *Materials and Methods*. Data are indicated as the mean ± SEM of seven mice in each group. *, $p < 0.05$. *D*, Histopathogical comparison of distal colon from mice injected with $CD4^+CD45RB^{high}$ alone, $CD4^+CD45RB^{high}$ + $CD4^+CD45RB^{low}$, $CD4^+CD45RB^{high}$ + $CD4^+GITR^+$, or $CD4^+GITR^-$. Original magnification, ×100. *E*, Histological scores were determined at 4 wk after transfer, as described in *Materials and Methods*. Data are indicated as the mean ± SEM of seven mice in each group. *, $p < 0.05$. *F*, LP cells and splenocytes were isolated at 4 wk after T cell transfer, and the number of $CD4^+$ cells was determined by flow cytometry. Data are indicated as the mean ± SEM of seven mice in each group. *, $p < 0.05$.

$GITR^+$ T cells using the well-described $CD4^+CD45RB^{high}$ T cell SCID-transferred colitis model (26). C.B-17 SCID mice were injected i.p. with one or two subpopulations of sorted $CD4^+$ T cell in PBS: 1) $CD4^+CD45RB^{high}$ alone (3×10^5 per body, as a positive control); 2) $CD4^+CD45RB^{high}$ + $CD4^+CD45RB^{low}$ (each 3×10^5 per body, as a negative control); 3) $CD4^+CD45RB^{high}$ + $CD4^+GITR^{high}$ (each 3×10^5 per body); or 4) $CD4^+GITR^{low}$ (3×10^5 per body) (Fig. 2*A*). The results clearly demonstrated that control of intestinal inflammation resided predominantly within $CD4^+GITR^+$ fraction, as these cells significantly inhibited the development of wasting disease and colitis (Fig. 2, *B–E*). Colons from mice reconstituted with a mixture of $CD4^+CD45RB^{high}$ and $CD4^+GITR^+$ cells exhibited no detectable pathological changes, and were indistinguishable from colons of mice reconstituted with a mixture of $CD4^+CD45RB^{high}$ + $CD4^+CD45RB^{low}$ cells (Fig. 2*D*). In contrast, mice reconstituted with $CD4^+CD45RB^{high}$ or $CD4^+GITR^-$ cells alone did develop wasting disease and severe colitis (Fig. 2, *B* and *D*). The clinical and histological scorings also confirmed these results (Fig. 2, *C* and *E*). A further quantitative evaluation of $CD4^+$ T cell infiltration was made by isolating LPMCs from the resected bowels. Only a few $CD4^+$ T cells were recovered from the colonic tissue of mice reconstituted with $CD4^+CD45RB^{high}$ and $CD4^+GITR^+$ cells as compared with mice reconstituted with $CD4^+CD45RB^{high}$ or $CD4^+GITR^-$ cells alone (Fig. 2*F*). Furthermore, the number of $CD4^+$ splenocytes from mice reconstituted with $CD4^+CD45RB^{high}$ and $CD4^+GITR^+$ cells was significantly less than that from mice reconstituted with $CD4^+CD45RB^{high}$ alone (Fig. 2*F*). Interestingly, $CD4^+GITR^-$-transferred mice developed more severe wasting disease as compared with mice transferred with $CD4^+CD45RB^{high}$ T cells (Fig. 2*B*), albeit histological scores of these mice were similar (Fig. 2*E*). Consistent with this, $CD4^+$ T cell recovery from spleen of $CD4^+GITR^-$-transferred mice was significantly higher than that of $CD4^+CD45RB^{high}$-transferred mice (Fig. 2*F*), indicating peripheral expansion of $CD4^+$ T cells of $CD4^+GITR^-$-transferred mice was more severe as compared with that of $CD4^+CD45RB^{high}$-transferred mice.

Development of chronic colitis by administration of anti-GITR mAb

Because of the involvement of GITR in regulatory T cell-mediated suppression (25), we next attempted to assess whether anti-GITR mAb (DTA-1) could abrogate the regulatory activity in intestinal inflammation, and induce a wasting disease in animals restored with a mixture of $CD4^+CD45RB^{high}$ and $CD4^+CD45RB^{low}$ T cell

fractions (Fig. 3*A*). As a positive control, mice restored with $CD4^+CD45RB^{high}$ T cells alone developed a wasting disease that became evident 3–5 wk postreconstitution (Fig. 3*B*) and showed clinical and histological evidence of severe chronic colitis (Fig. 3, *C–E*). As a negative control, mice restored with both $CD4^+CD45RB^{high}$ and $CD4^+CD45RB^{low}$ T cell populations and administrated with control IgG by i.p. injection (1 mg weekly up to 6 wk) did not develop wasting disease and colitis at all (Fig. 3, *B–E*). In contrast, administration of anti-GITR mAb (DTA-1) to mice restored with both $CD4^+CD45RB^{high}$ and $CD4^+CD45RB^{low}$ T cell populations by i.p. injection (1 mg weekly up to 6 wk) induced, by 4 wk after T cell transfer, wasting disease (Fig. 3, *B* and *C*) and showed histological evidence of chronic intestinal inflammation (Fig. 3, *D* and *E*). In addition, LP $CD4^+$ T cells from mice transferred with both $CD4^+CD45RB^{high}$ and $CD4^+CD45RB^{low}$ T cell populations with DTA-1 administration produced significantly more IFN-γ as compared with those from mice transferred with both $CD4^+CD45RB^{high}$ and $CD4^+CD45RB^{low}$ T cell populations with control IgG administration (data not shown). In contrast, production of IL-4 or IL-10 was not significantly affected (data not shown).

$CD4^+CD25^-GITR^+$ as well as $CD4^+CD25^+GITR^+$ T cells inhibited the development of classical $CD4^+CD45RB^{high}$-transferred colitis

Having evidence that the $CD4^+GITR^+$ T cell population has regulatory activity in vivo, and $CD4^+GITR^+$ T cells also exist in $CD4^+CD25^-$ subpopulation, we sorted strictly $CD4^+GITR^+$ T cells into $CD4^+CD25^+GITR^+$ and $CD4^+CD25^-GITR^+$ T cell fractions, and tested for their ability to inhibit the colitis induced by transfer of $CD4^+CD45RB^{high}$ cells (Fig. 4*A*). Mice restored with the $CD4^+CD45RB^{high}$ subset alone developed a wasting disease and severe chronic colitis (Fig. 4, *B* and *C*). The results clearly demonstrated that regulation of intestinal inflammation resided predominantly within both the $CD4^+CD25^+GITR^+$ and $CD4^+CD25^-GITR^+$ fractions, as these cells significantly inhibited the development of wasting disease and colitis (Fig. 4, *B–E*), although the wasting disease by the cotransfer of $CD4^+CD25^+GITR^+$ T cells was significantly milder than that by the cotransfer of $CD4^+CD25^-GITR^+$ T cells, as indexed by the percentage of weight changes (Fig. 4*B*). However, the clinical and histological scores, the suppression of LP $CD4^+$ T cell infiltration, and IFN-γ production by LP $CD4^+$ T cells from mice cotransferred with $CD4^+CD25^-GITR^+$ were apt to be milder, but not significant when compared with mice cotransferred with $CD4^+CD25^+GITR^+$ T cells (Fig. 4, *C–G*). This indicates that regulatory T cells are not only present in $CD4^+CD25^-GITR^+$ T cell population as well as $CD4^+CD25^+GITR^+$ T cell population in vivo, but also dependent on the expression of GITR rather than that of CD25.

Characterization of $CD4^+CD25^+GITR^+$ and $CD4^+CD25^-GITR^+$ T cells in terms of regulatory T cell in vitro

We finally explored whether $CD4^+CD25^-GITR^+$ subset retains regulatory activity in vitro. Unfractionated $CD4^+$, $CD4^+CD25^+GITR^+$, and $CD4^+CD25^+GITR^+$ T cells were sorted (Fig. 5*A*). Recently, it has been shown that resting regulatory $CD4^+CD25^+$ T cells intracellularly express CTLA-4 (13, 14). Thus, we analyzed intracellular expression of this marker on freshly isolated $CD4^+CD25^+GITR^+$ and $CD4^+CD25^-GITR^+$ T cells. As shown in Fig. 5*A*, $CD4^+CD25^-GITR^+$ T cells as well as

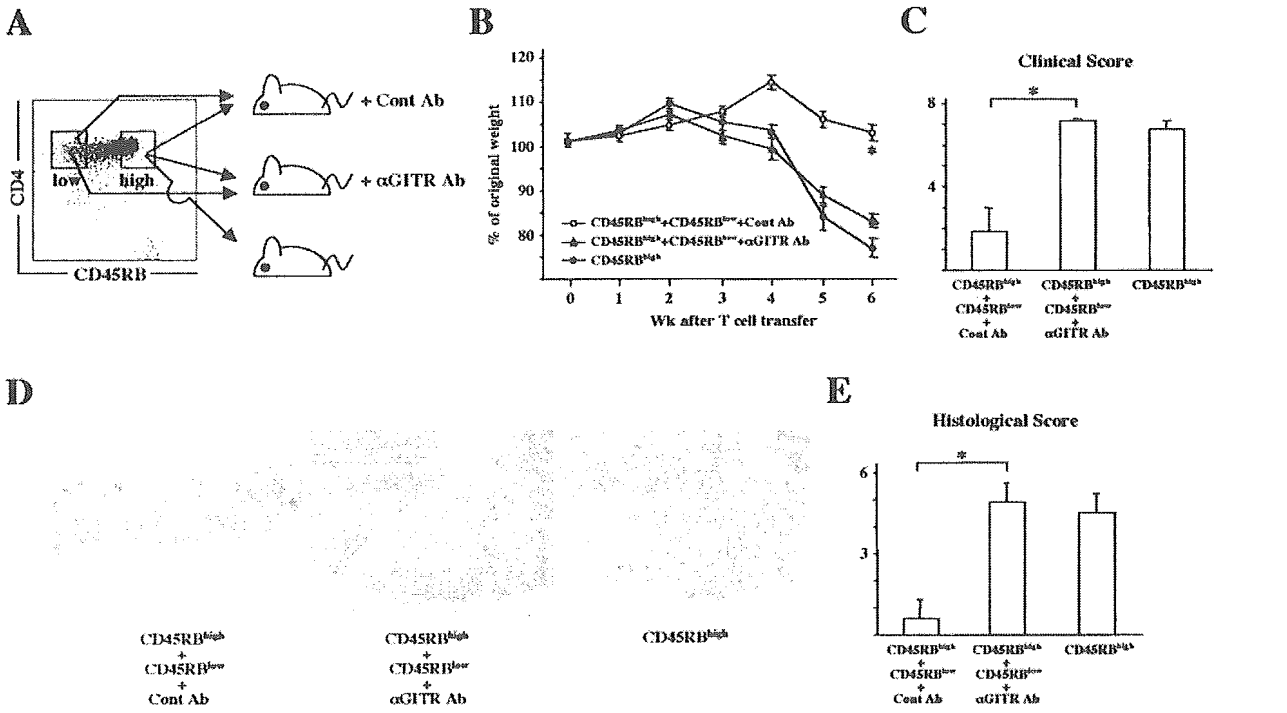

FIGURE 3. Development of chronic colitis by administration of anti-GITR mAb. *A*, C.B-17 SCID mice were injected i.p. with $CD4^+CD45RB^{high}$ + $CD4^+CD45RB^{low}$ T cells (each 3×10^5 per body), and also were given 1 mg control rat IgG or anti-GITR (DTA-1) mAb by i.p. injection weekly from the day of T cell transfer over a period of 6 wk. As a positive control, C.B-17 SCID mice were injected i.p. with $CD4^+CD45RB^{high}$ T cells alone (3×10^5 per body) (six animals per each group). *B*, Administration of anti-GITR mAb to mice reconstituted with a mixture of $CD4^+CD45RB^{high}$ + $CD4^+CD45RB^{low}$ T cells induced a severe wasting disease. *C*, Clinical scores were determined at 6 wk after transfer, as described in *Materials and Methods*. Data are indicated as the mean ± SEM of six mice in each group. *, $p < 0.05$. *D*, Histopathological comparison of distal colon from each mice group. Original magnification, ×100. *E*, Histological scores were determined at 6 wk after transfer, as described in *Materials and Methods*. Data are indicated as the mean ± SEM of six mice. *, $p < 0.05$.

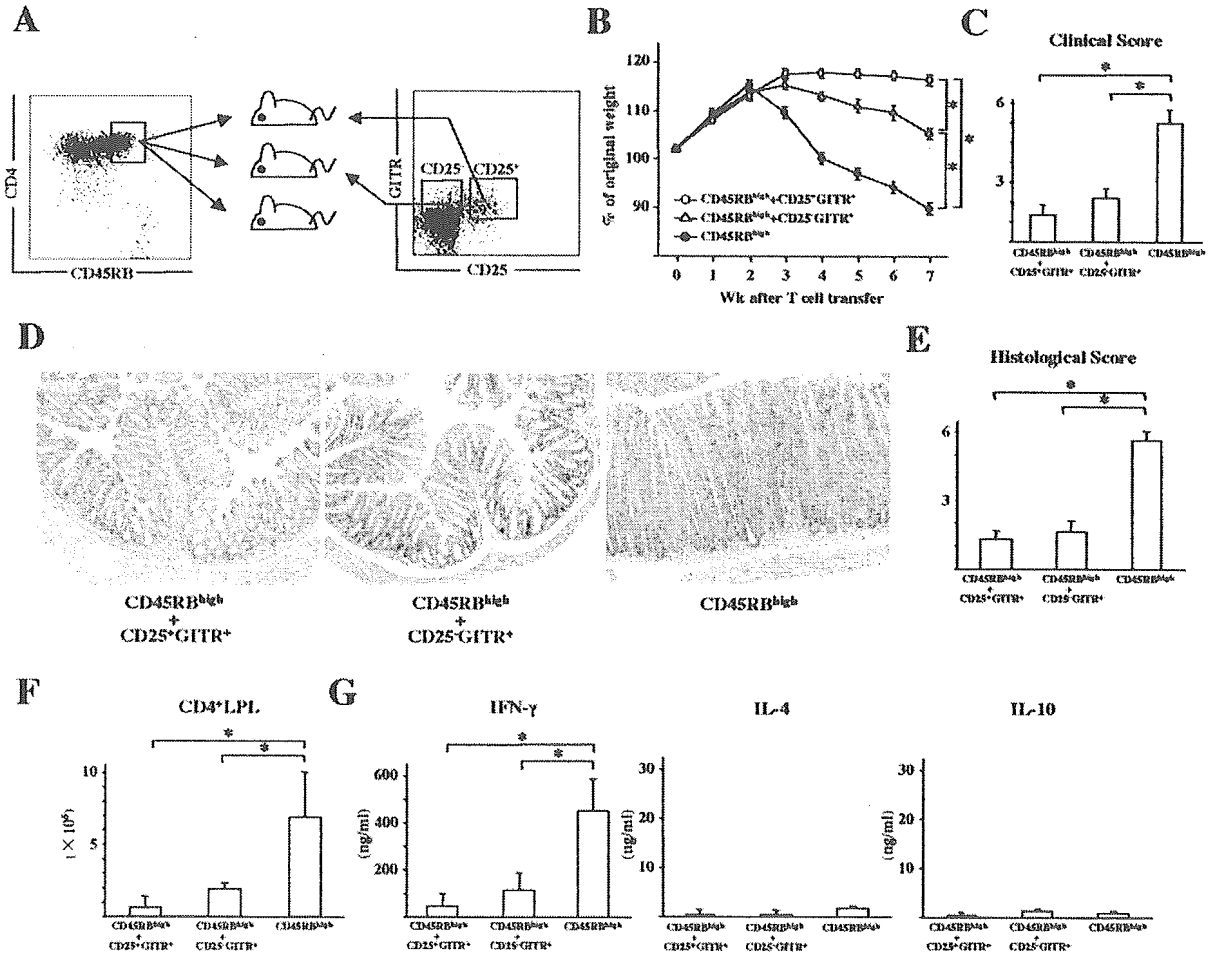

FIGURE 4. $CD4^+CD25^-GITR^+$ as well as $CD4^+CD25^+GITR^+$ T cells inhibited development of the classical $CD4^+CD45RB^{high}$-transferred colitis. *A*, C.B-17 SCID mice were injected i.p. with: 1) $CD4^+CD45RB^{high}$ (3×10^5 per body) + $CD4^+CD25^+GITR^+$ T cells (1×10^5 per body); 2) $CD4^+CD45RB^{high}$ (3×10^5 per body) + $CD4^+CD25^-GITR^+$ T cells (1×10^5 per body); or 3) $CD4^+CD45RB^{high}$ T cells alone (3×10^5 per body, as a positive control) (seven animals per each group). *B*, $CD4^+CD25^-GITR^+$ T cells inhibited a wasting disease as well as $CD4^+CD25^+GITR^+$ cells. Recipient SCID mice were weighed on the day of T cell transfer and three times per week thereafter; △, $CD4^+CD45RB^{high}$ + $CD4^+CD25^+GITR^+$ cells; □, $CD4^+CD45RB^{high}$ + $CD4^+CD25^-GITR^+$ cells; ●, $CD4^+CD45RB^{high}$ alone. Statistical analysis was performed to compare the slopes of the weight change between the groups of mice that received $CD4^+CD45RB^{high}$ + $CD4^+CD25^+GITR^+$ or $CD4^+CD45RB^{high}$ + $CD4^+CD25^-GITR^+$ T cells with mice that received $CD4^+CD45RB^{high}$ T cells. *, $p < 0.05$. *C*, $CD4^+CD25^-GITR^+$ T cells inhibited a chronic colitis as well as $CD4^+CD25^+GITR^+$ T cells. Clinical scores were determined at 7 wk after transfer, as described in *Materials and Methods*. Data are indicated as the mean ± SEM of seven mice in each group. *, $p < 0.05$. *D*, Histopathology of distal colon from mice injected with $CD4^+CD45RB^{high}$ + $CD4^+CD25^+GITR^+$ T cells, $CD4^+CD45RB^{high}$ + $CD4^+CD25^-GITR^+$ T cells, or $CD4^+CD45RB^{high}$ T cells alone. Original magnification, ×100. *E*, Histological scores were determined at 7 wk after transfer, as described in *Materials and Methods*. Data are indicated as the mean ± SEM of seven mice in each group. *, $p < 0.05$. *F*, LP cells were isolated from the colon at 7 wk after T cell transfer, and the number of $CD4^+$ cells was determined by flow cytometry. Data are indicated as the mean ± SEM of seven mice in each group. *, $p < 0.05$. *G*, LP $CD4^+$ T cells were isolated from mice reconstituted with $CD4^+CD45RB^{high}$ + $CD4^+CD25^+GITR^+$ T cells, $CD4^+CD45RB^{high}$ + $CD4^+CD25^-GITR^+$ T cells, or $CD4^+CD45RB^{high}$ T cells alone (1×10^5/well), and were incubated in the presence of coated anti-CD3ε (5 μg/ml) and anti-CD28 mAb (2 μg/ml). After 48 h of culture, the supernatants were harvested and analyzed for IFN-γ, IL-4, and IL-10 by ELISA. *, $p < 0.05$.

$CD4^+CD25^+GITR^+$ cells expressed elevated levels of CTLA-4 intracellularly, but this was expressed on only 0.5% of unfractionated $CD4^+$ cells. $CD4^+CD25^-GITR^+$ subsets were found to be hyporesponsive to stimulation with Con A (5 μg/ml) as compared with unfractionated $CD4^+$ T cells (Fig. 5*B*), albeit more proliferative than $CD4^+CD25^+GITR^+$ counterparts, indicating both $CD4^+CD25^+GITR^+$ and $CD4^+CD25^-GITR^+$ T cells were anergic. However, the addition of 100 U/ml exogenous IL-2 to the cultures with $CD4^+CD25^+GITR^+$ T cells, but not $CD4^+CD25^-GITR^+$ T cells, partially overcame the proliferative defect, suggesting that CD25 is a functional receptor for $CD4^+CD25^+GITR^+$ regulatory T cells (Fig. 5*B*). Furthermore, $CD4^+CD25^-GITR^+$ T cells were able to suppress the proliferation of $CD4^+$ cells when cocultured in vitro, albeit less potent than that of their $CD4^+CD25^+GITR^+$ counterparts (Fig. 5*C*), indicating that $CD4^+CD25^-GITR^+$ T cells were also regulatory. Finally, supernatants after in vitro stimulation with anti-CD3/CD28 mAbs were analyzed by ELISA. As shown in Fig. 5*D*, unfractionated $CD4^+$ cells produced IFN-γ, IL-4, IL-2, and IL-10, but not TGF-β, whereas $CD4^+CD25^+GITR^+$ cells and $CD4^+CD25^-GITR^+$ cells produced less amounts of IFN-γ and IL-4, but significantly higher levels of IL-10 and TGF-β as compared with whole $CD4^+$ T cells. Interestingly, $CD4^+CD25^-GITR^+$ T cells produced significantly higher level of IL-2 than $CD4^+CD25^+GITR^+$ cells. These findings demonstrate $CD4^+CD25^-GITR^+$ T cells as well as $CD4^+CD25^+GITR^+$ cells are phenotypically and functionally identical with regulatory T cells in vitro, although the data of cytokine production are yet controversial.

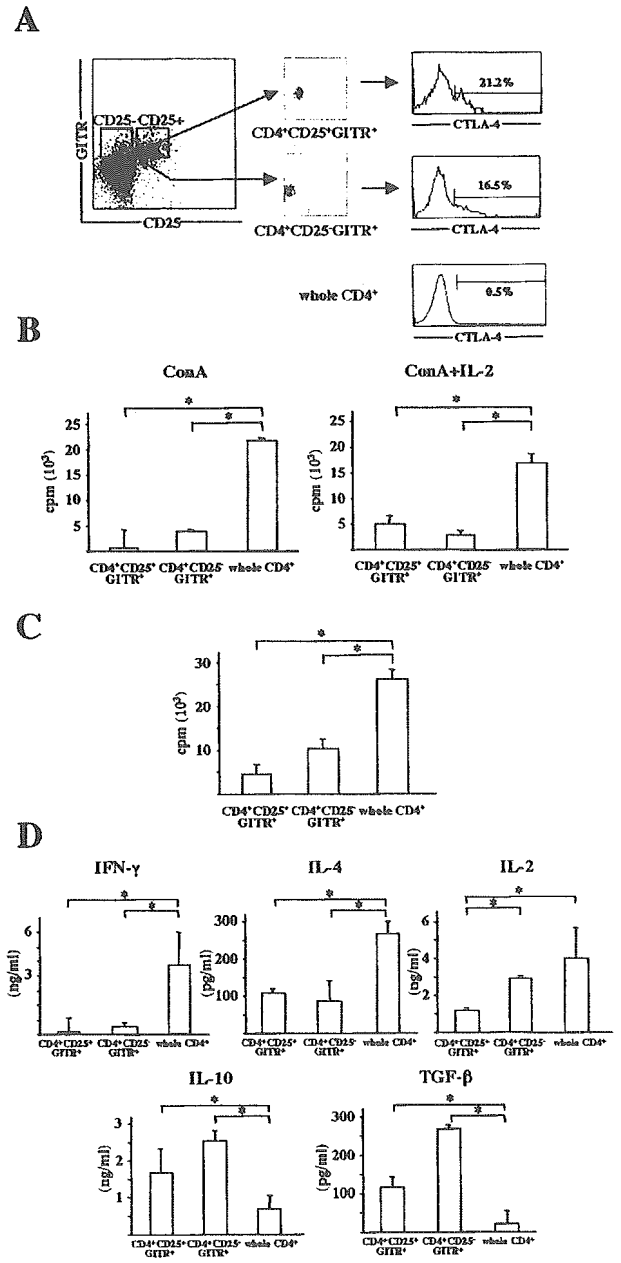

FIGURE 5. Characterization of $CD4^+CD25^+GITR^+$ and $CD4^+CD25^-GITR^+$ T cells in terms of regulatory T cell in vitro. *A*, $CD4^+CD25^-GITR^+$ T cells express CTLA-4 intracellularly as well as $CD4^+CD25^+GITR^+$ T cells. $CD4^+CD25^+GITR^+$ T cells, $CD4^+CD25^-GITR^+$ T cells, and unfractionated $CD4^+$ T cells were stained for intracellular CTLA-4 expression and analyzed on the flow cytometry. *B*, Proliferation of $CD4^+CD25^+GITR^+$, $CD4^+CD25^-GITR^+$, and unfractionated $CD4^+$ T cells. Cells were stimulated for 72 h with 5 μg/ml Con A or 5 μg/ml Con A + human rIL-2 (100 U/ml) in the presence of irradiated $CD4^-$ splenocytes as APCs. In the experiment shown, which is representative of two individuals, the counts correspond to [^{3}H]thymidine incorporation during the final 9 h of a 72-h culture. *, $p < 0.05$. *C*, Both $CD4^+CD25^+GITR^+$ and $CD4^+CD25^-GITR^+$ subsets suppress the proliferation of $CD4^+$ T cells in vitro. $CD4^+$ T cells and sorted $CD4^+CD25^+GITR^+$ or $CD4^+CD25^-GITR^+$ T cells were cocultured for 72 h with Con A (3 μg/ml) at a 1:2 ratio in the presence of APCs. *, $p < 0.05$. *D*, Cytokine production by $CD4^+CD25^+GITR^+$ and $CD4^+CD25^-GITR^+$, and unfractionated $CD4^+$ T cells. Purified $CD4^+CD25^+GITR^+$ and $CD4^+CD25^-GITR^+$, and unfractionated $CD4^+$ T cells (1×10^5/well) were incubated with plate-bound anti-CD3 (10 μg/ml) and anti-CD28 (5 μg/ml) mAbs. Supernatants were collected after 24 h for IL-2; 48 h for IL-4, IL-10, and IFN-γ; and 72 h for TGF-β. Results (means ± SD) are representative of three independent experiments. *, $p < 0.05$.

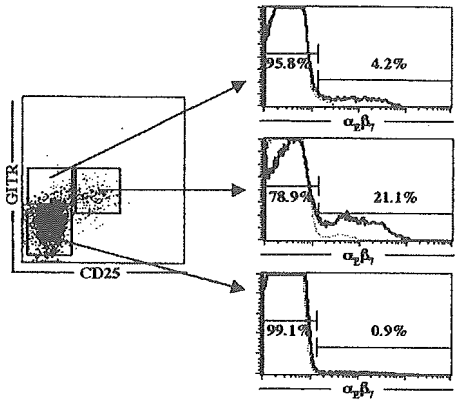

FIGURE 6. Expression of α_E integrin on $CD4^+CD25^-GITR^+$, $CD4^+CD25^+GITR^+$, and $CD4^+GITR^-$ T cells from spleen. Freshly isolated splenic $CD4^+$ T cells by anti-CD4 MACS beads were stained with anti-CD25, anti-GITR, and anti-α_E mAb.

Correlation between $CD4^+CD25^-GITR^+$ cells and other $CD25^-$ regulatory cells

Because Lehmann et al. (22) have recently demonstrated that $CD4^+CD25^-$ α_E^+ (integrin $\alpha_E\beta_7$) T cells in periphery display regulatory activity in vivo and in vitro, we then asked whether the expression of GITR has a correlation with that of α_E. As shown in Fig. 6, most of $CD4^+CD25^-GITR^+$ T cells were not within α_E^+ fraction, although very small part of these cells expressed α_E (4.3 ± 0.9% in whole $CD4^+CD25^-GITR^+$ T cells), indicating the GITR marker for regulatory T cell does not correlate with expression of α_E. Consistent with the previous report (22), we also found that most of $CD4^+CD25^+GITR^+$ T cells did not express α_E (20.9 ± 5.9% in whole $CD4^+CD25^+GITR^+$ T cells) (Fig. 6). Based on another evidence that NKT cells are $CD25^-$ (34), and also possess regulatory function in some autoimmune disease models, such as diabetes model (35, 36), we next asked whether our $CD4^+CD25^-GITR^+$ cells derived from C57BL/6 mice express NK 1.1, which is one of NKT markers. However, both $CD4^+CD25^+GITR^+$ and $CD4^+CD25^-GITR^+$ cells did not express NK 1.1 (data not shown), indicating our cells were not NKT cells. Additionally, we confirmed that $CD4^+CD25^-GITR^+$ cells were also $DX5^-$ (data not shown), indicating our cells were neither NKT nor NK cells. Finally, we asked whether $CD4^+CD25^-$ $GITR^+$ T cells really express TCR$\alpha\beta$, because it has become clear that TCR$\gamma\delta^+$ T cells play a key role in the regulation of mucosal immunity (37). However, all $CD4^+CD25^-GITR^+$ cells as well as $CD4^+CD25^+GITR^+$ cells were TCR$\alpha\beta^+$, but not TCR$\gamma\delta^+$. Taken together with these results, our $CD4^+CD25^-GITR^+$ regulatory T cells should be a novel and unique subset, although $CD4^+CD25^-\alpha_E^+$ cells may overlap a small part of $CD4^+CD25^-$ $GITR^+$ regulatory T cells.

Discussion

In the present study, we demonstrated that both $CD4^+CD25^+$ $GITR^+$ and $CD4^+CD25^-GITR^+$ T cells, regardless of the CD25 expression, prevented the development of colitis, indicating $CD4^+CD25^-GITR^+$ T cells as well as $CD4^+CD25^+GITR^+$ T cells retain the regulatory function.

At present, useful regulatory T cell surface markers for the discrimination between functional subsets of $CD4^+$ cells are CD25 (12), CD45RB (26), α_E integrin (22), and GITR (25). The majority of the $CD4^+CD25^+$ cells were $CD45RB^{low}$ and also $GITR^+$ (Fig. 1). It is widely accepted that $CD4^+CD25^+$ T cells are the major population to contain regulatory T cells in several experimental

systems. Hence, the relationship between $CD4^+CD25^+$ and $CD4^+CD45RB^{low}$ regulatory T cell subsets is not well established. In addition, there is increasing evidence that regulatory $CD4^+$ T cells exist in the $CD25^-$ compartment as well (19, 22, 24). Although Shimizu et al. (25) have shown that GITR is indeed predominantly expressed on $CD4^+CD25^+$ spleen cells, as previously described, we found that a part of $CD4^+CD25^-$ T cells also expressed GITR, whereas most of $CD4^+CD25^-$ T cells did not (Fig. 1), raising a question of whether $CD4^+CD25^-GITR^+$ T cells play any useful part in protective immune responses as regulatory T cells. In fact, we demonstrated that $CD4^+CD25^-GITR^+$ T cells were anergic and regulatory, expressed CTLA-4 intracellularly, and produced both IL-10 and TGF-β in vitro (Fig. 5), indicating these cells should be regulatory T cells. As expected, $CD4^+CD25^-GITR^+$ T cells also inhibited the development of wasting disease and colitis in vivo (Fig. 4). Taken together with the fact that administration of anti-GITR mAb induced chronic colitis in mice restored with both $CD4^+CD45RB^{high}$ and $CD4^+CD45RB^{low}$ T cells (Fig. 3), the present studies could demonstrate that $CD4^+CD45RB^{low}$ subset of regulatory T cells expresses GITR.

These observations raise another question of the relationship between $CD25^+$ and $CD25^-$ regulatory $CD4^+$ T cells and the origin of these cells. At this point, we cannot exclude that the two subsets differ in their development, function, and/or specificity. It is possible that regulatory $CD25^-$ T cells are descendants of thymic regulatory $CD25^+$ T cells, and represent an alternative state of the same functional pool of peripheral regulatory T cells. Although further study is needed to address this, $CD4^+CD25^+$ T cells might be enriched for regulatory T cells simply because they are activated (effector state), and might become $CD25^-$ T cells in the absence of the appropriate stimuli (memory state). If so, GITR might strictly maintain to suppress the regulatory function in the resting conditions, because GITR signaling is shown to abolish regulatory function. Accordingly, GITR might be more reliable surface marker for regulatory T cells because both $CD4^+CD25^-$ and $CD4^+CD25^+$ regulatory T cells retain GITR expression. Furthermore, this hypothesis seems to be favorable for the reason that $CD4^+CD25^-GITR^+$ regulatory T cells retain less potent regulatory function as compared with $CD4^+CD25^+GITR^+$ T cells (Fig. 5).

However, it is also well known that the transfer of $CD4^+CD45RB^{high}$ T cells into syngeneic athymic nude mice does not induce the development of wasting disease and colitis (38), whereas the transfer into syngeneic SCID mice does (26). This contrasting evidence strongly suggests that there exists some regulatory T cell compartment in recipient athymic nude mice to protect the development of colitis. Indeed, several lines of evidence suggest that some extrathymic TCR$\alpha\beta$ T cells also exist in athymic nude mice (39, 40). These cells appear relatively late in ontogeny, randomly increase in numbers as a function of age, and encompass $CD4^-CD8^-$, $CD4^+CD8^-$, and $CD4^-CD8^+$ cells. In fact, one possible pathway of extrathymic selection of $CD4^+CD25^-$ regulatory T cells has been demonstrated by elegant studies in which mice expressing a transgenic TCR that recognizes an influenza hemagglutinin (HA) peptide were crossed to two lineages expressing the HA peptide under the control of different promoters (21). In this study, expression of HA Ag by thymic epithelial cells produced mostly $CD4^+CD25^+$ regulatory T cells. In contrast, expression of HA Ag by nonactivated hemopoietic cells produced mostly $CD4^+CD25^-$ regulatory T cells even in the absence of a functioning thymus. This indicates that distinct pathways can be exploited to interfere with unwanted immune responses. If so, some $CD4^+$ T cells in athymic nude mice might retain regulatory function. Alternatively, it is also possible that SCID mice are poorly equipped to face DNA damage (DNA double-strand break repair system) induced by inflammation in the intestinal mucosa compared with nude mice (41, 42). Further study will be needed to determine whether the origin of $CD4^+CD25^-GITR^+$ T cells is thymic or extrathymic.

Studies in various animal models provide strong evidence of a role for cytokines in the effector function of regulatory T cells in vivo; however, the cytokines involved vary depending on the model. In SCID-transferred IBD model, protection from colitis does not require IL-4, but is crucially dependent on TGF-β and IL-10 production by T cells (17). Consistent with this, $CD4^+CD25^-GITR^+$ T cells as well as $CD4^+CD25^+GITR^+$ T cells produced significant levels of IL-10 and TGF-β, but not IL-4. Further investigation will be needed to address whether neutralizing anti-IL-10R and anti-TGF-β mAbs abrogate the protective effect of $CD4^+CD25^-GITR^+$ T cells in vivo.

In a recent publication, Lehmann and colleagues (22) reported that the integrin $\alpha_E\beta_7$, which recognizes epithelial cadherin, identified the most potent subpopulation of regulatory $CD4^+CD25^+$ T cells. In addition, they showed that $CD4^+CD25^-\alpha_E^+$ T cells displayed to protect the development of the SCID-transferred colitis, and also possessed regulatory function in vitro. However, it should be emphasized that these cells and our $CD4^+CD25^-GITR^+$ T cells are distinct subpopulations of each other. Most importantly, $CD4^+CD25^-GITR^+$ T cells produced fewer amounts of IFN-γ and IL-4, although $CD4^+CD25^-\alpha_E^+$ T cells did produce large amounts of these cytokines. Second, CD25 could be expressed on both α_E^+ and α_E^- T cells, while it was expressed on only $GITR^+$ T cells. Third, the ratio of $CD4^+CD25^-\alpha_E^+$ T cells to total of $CD4^+CD25^+\alpha_E^+$, $CD4^+CD25^+\alpha_E^-$, and $CD4^+CD25^-\alpha_E^+$ was quite small, when compared with the ratio of $CD4^+CD25^-GITR^+$ T cells to total of $CD4^+CD25^+GITR^+$ and $CD4^+CD25^-GITR^+$ T cells. Fourth, it is well known that one-third of lamina propria $CD4^+$ T cells from normal mice express $\alpha_E\beta_7$ integrin (44), while the population of $GITR^+$ LP $CD4^+$ T cells is rather less (5–10% in $CD4^+$ T cells; data not shown), similarly to that of splenic $CD4^+$ T cells (Fig. 1). Finally, it has been reported that α_E-deficient mice developed autoimmune disease in skin (45); however, GITR-deficient mice did not (46), indicating α_E might be needed to maintain regulatory function, but conversely, GITR may be needed to suppress regulatory function. Taken together, these results support that GITR expresses on $CD4^+$ T cells in independent manner with the expression of $\alpha_E\beta_7$ integrin.

In conclusion, we showed that $CD4^+GITR^+$ T cell population, regardless of CD25 expression, should contain regulatory T cells. The evidence in this study may provide not only a clue of the exact correlation between $CD4^+CD45RB^{low}$ and $CD4^+CD25^+$ regulatory T cells, but also the tool to investigate the origin of $CD4^+CD25^+$ and $CD4^+CD25^-$ regulatory T cells. Furthermore, the present study suggests that GITR could be beneficial as a specific marker for regulatory T cells controlling mucosal inflammation and as a target for treatment of IBD.

Acknowledgments

We express special thanks to Drs. Shimon Sakaguchi and Masahiro Ono for critical comments, and Hiroshi Nishikawa for technical assistance.

References

1. Holmgren, J., and A. Rudin. 1999. Mucosal immunity and bacteria. In *Mucosal Immunology*. P. L. Ogra, M. E. Lamm, J. Bienenstock, J. Mestecky, W. Strober, and J. R. McGhee, eds. Academic Press, San Diego, p. 685.
2. Asseman, C., S. Fowller, and F. Powrie. 2000. Control of experimental inflammatory bowel disease by regulatory T cells. *Am. J. Respir. Crit. Care Med. 162:S185.*
3. Abbas, A. K., K. M. Murphy, and A. Sher. 1996. Functional diversity of helper T lymphocytes. *Nature 383:787.*
4. O'Garra, A. 1998. Cytokines induce the development of functionally heterogenous T helper cell subsets. *Immunity 8:275.*

5. Gershon, R. K. 1975. A disquisition on suppressor T cells. *Transplant. Rev. 26:170.*
6. Sakaguchi, S., N. Sakaguchi, J. Shimizu, S. Yamazaki, T. Sakihama, M. Itoh, Y. Kuniyasu, T. Nomura, M. Toda, and T. Takahashi. 2001. Immunologic tolerance maintained by $CD25^+$ $CD4^+$ regulatory T cells: their common role in controlling autoimmunity, tumor immunity, and transplantation tolerance. *Immunol. Rev. 182:18.*
7. Curotto de Lafaille, M. A., and J. J. Lafaille. 2002. $CD4^+$ regulatory T cells in autoimmunity and allergy. *Curr. Opin. Immunol. 14:771.*
8. Powrie, F., and M. W. Leach. 1995. Genetic and spontaneous models of inflammatory bowel disease in rodents: evidence for abnormalities in mucosal immune regulation. *Ther. Immunol. 2:115.*
9. Blumberg, R. S., L. J. Saubermann, and W. Strober. 1999. Animal models of mucosal inflammation and their relation to human inflammatory bowel disease. *Curr. Opin. Immunol. 11:648.*
10. Strober, W., I. J. Fuss, and R. S. Blumberg. 2002. The immunology of mucosal models of inflammation. *Annu. Rev. Immunol. 20:495.*
11. Maloy, K., and F. Powrie. 2001. Regulatory T cells in the control of immune pathology. *Nat. Immun. 2:816.*
12. Sakaguchi, S., N. Sakaguchi, M. Asano, M. Itoh, and M. Toda. 1995. Immunological self-tolerance maintained by acute T cells expressing IL-2 receptor α chains (CD25): breakdown of a single mechanism of self-tolerance causes various autoimmune diseases. *J. Immunol. 155:1151.*
13. Shevach, E. M. 2002. $CD4^+CD25^+$ suppressor T cells: more questions than answers. *Nat. Rev. Immunol. 2:389.*
14. Battaglia, M., B. R. Blazar, and M. G. Roncarolo. 2002. The puzzling world of murine T regulatory cells. *Microbes Infect. 4:559.*
15. Sakaguchi, S. 2000. Regulatory T cells: key controllers of immunological self-tolerance. *Cell 101:455.*
16. Sakaguchi, S., T. Takahashi, S. Yamazaki, Y. Kuniyasu, M. Itoh, N. Sakaguchi, and J. Shimizu. 2001. Immunologic self tolerance maintained by T-cell-mediated control of self-reactive T cells: implications for autoimmunity and tumor immunity. *Microbes Infect. 3:911.*
17. Read, S., V. Malmstrom, and F. Powrie. 2000. Cytotoxic T lymphocyte-associated antigen 4 plays an essential role in the function of $CD4^+CD25^+$ regulatory cells that control intestinal inflammation. *J. Exp. Med. 193:295.*
18. Takahashi, T., T. Tagami, S. Yamazaki, T. Ueda, J. Shimizu, N. Sakaguchi, T. W. Mak, and S. Sakaguchi. 2000. Immunologic self-tolerance maintained by $CD4^+CD25^+$ regulatory T cells constitutively expressing cytotoxic T lymphocyte-associated antigen 4. *J. Exp. Med. 193:303.*
19. Graca, L., S. Thompson, C. Y. Lin, E. Adams, S. P. Cobbold, and H. Waldmann. 2002. Both $CD4^+CD25^+$ and $CD4^+CD25^-$ regulatory cells mediate dominant transplantation tolerance. *J. Immunol. 168:5558.*
20. Van de Keere, F., and S. Tonegawa. 1998. $CD4^+$ T cells prevent spontaneous experimental autoimmune encephalomyelitis in anti-myelin basic protein T cell receptor transgenic mice. *J. Exp. Med. 188:1875.*
21. Apostolou, I., A. Sarukhan, L. Klein, and H. von Boehmer. 2002. Origin of regulatory T cells with known specificity for antigen. *Nat. Immun. 3:756.*
22. Lehmann, J., J. Huehn, M. de la Rosa, F. Maszyna, U. Kretschmer, V. Krenn, M. Brunner, and A. Hamann. 2002. Expression of the integrin $\alpha_E\beta_7$ identifies unique subsets of $CD25^+$ as well as $CD25^-$ regulatory T cells. *Proc. Natl. Acad. Sci. USA 99:13031.*
23. Stephens, L. A., and D. Mason. 2000. CD25 is a marker for $CD4^+$ thymocytes that prevent autoimmune diseases in rats, but peripheral T cells with this function are found in both $CD25^+$ and $CD25^-$ subpopulations. *J. Immunol. 165:3105.*
24. Annacker, O., R. Pimenta-Araujo, O. Burlen-Defranoux, T. C. Barbosa, A. Cumano, and A. Bandeira. 2001. $CD25^+CD4^+$ T cells regulate the expansion of peripheral CD4 T cells through the production of IL-10. *J. Immunol. 166:3008.*
25. Shimizu, J., S. Yamazaki, T. Takahashi, Y. Ishida, and S. Sakaguchi. 2002. Stimulation of $CD25^+CD4^+$ regulatory T cells through GITR breaks immunological self-tolerance. *Nat. Immun. 3:135.*
26. Powrie, F., M. W. Leach, S. Mauze, L. B. Caddle, and R. L. Coffman. 1993. Phenotypically distinct subsets of $CD4^+$ T cells induce or protect from chronic intestinal inflammation in C.B-17 *scid* mice. *Int. Immunol. 5:1461.*
27. Totsuka, T., T. Kanai, R. Iiyama, K. Uraushihara, M. Yamazaki, R. Okamoto, T. Hibi, K. Tezuka, M. Azuma, H. Akiba, et al. 2003. 27. Ameliorating effect of anti-inducible costimulator monoclonal antibody in a murine model of chronic colitis. *Gastroenterology 119:715.*
28. Liu, Z., K. Geboes, S. Colpaert, L. Overbergh, C. Mathieu, H. Heremans, M. de Boer, L. Boon, G. D'haens, P. Rutgeerts, and J. L. Ceuppens. 2000. Prevention of experimental colitis in SCID mice reconstituted with $CD45RB^{high}CD4^+$ T cells by blocking the CD40-CD154 interactions. *J. Immunol. 164:6005.*
29. Kanai, T., M. Watanabe, A. Okazawa, T. Sato, M. Yamazaki, S. Okamoto, H. Ishii, T. Totsuka, R. Iiyama, R. Okamoto, et al. 2001. Macrophage-derived IL-18-mediated intestinal inflammation in the murine model of Crohn's disease. *Gastroenterology 121:875.*
30. Stephens, L. A., C. Mottet, D. Mason, and F. Powrie. 2001. Human $CD4^+CD25^+$ thymocytes and peripheral T cells have immune suppressive activity in vitro. *Eur. J. Immunol. 31:1247.*
31. Dieckmann, D., H. Plottner, S. Berchtold, T. Berger, and G. Schuler. 2001. Ex vivo isolation and characterization of $CD4^+CD25^+$ T cells with regulatory properties from human blood. *J. Exp. Med. 193:1303.*
32. Levings, M. K., R. Sangregorio, and M. G. Roncarolo. 2001. Human $CD25^+CD4^+$ T regulatory cells suppress naive and memory T cell proliferation and can be expanded in vitro without loss of function. *J. Exp. Med. 193:1295.*
33. Jonuleit, H., E. Schmitt, M. Stassen, A. Tuettenberg, J. Knop, and A. H. Enk. 2001. Identification and functional characterization of human $CD4^+CD25^+$ T cells with regulatory properties isolated from peripheral blood. *J. Exp. Med. 193:1285.*
34. Vicari, A. P., and A. Zlotnik. 1996. Mouse NK 1.1^+ T cells: a new family of T cells. *Immunol. Today 17:71.*
35. Hong, S., M. T. Wilson, I. Serizawa, L. Wu, N. Singh, O. V. Naidenko, T. Miura, T. Haba, D. C. Scherer, I. Wei, et al. 2001. The natural killer T-cell ligand α-galactosylceramide prevents autoimmune diabetes in non-obese diabetic mice. *Nat. Med. 7:1052.*
36. Beaudoin, L., V. Laloux, J. Novak, B. Lucas, and A. Lehuen. 2002. NKT cells inhibit the onset of diabetes by impairing the development of pathogenic T cells specific for pancreatic β cells. *Immunity 17:725.*
37. Yamamoto, M., and H. Kiyono. 1999. Immunoregulatory functions of mucosal $\gamma\delta$ T cells. *Microbes Infect. 1:241.*
38. Laroux, S., and M. B. Grisham. 2002. Activated/memory but not naive $CD4^+$ T cells induce chronic colitis in athymic nude mice. In *11th International Congress of Mucosal Immunology, Mucosal Immunology Update, June 16.* C. O. Elson, ed. Bethesda, MD: Society for Mucosal Immunology. 10:1640 (Abstr.).
39. Hunig, T. 1983. T-cell function and specificity in athymic mice. *Immunol. Today 4:84.*
40. MacDonald, H. R. 1984. Phenotypic and functional characteristics of "T-like" cells in nude mice. *Exp. Cell Biol. 52:2.*
41. Blunt, T., N. J. Finnie, G. E. Taccioli, G. C. Smith, J. Demengeot, T. M. Gottlieb, R. Mizuta, A. J. Varghese, F. W. Alt, P. A. Jeggo, and S. P. Jackson. 1995. Defective DNA-dependent protein kinase activity is linked to V(D)J recombination and DNA repair defects associated with the murine *scid* mutation. *Cell 80: 813.*
42. Fulop, G. M., and R. A. Phillips. 1990. The *scid* mutation in mice causes a general defect in DNA repair. *Nature 347:479.*
43. Cepek, K. L., S. K. Shaw, C. M. Parker, G. J. Russell, J. S. Morrow, D. L. Rimm, and M. B. Brenner. 1994. Adhesion between epithelial cells and T lymphocytes mediated by E-cadherin and $\alpha_E\beta_7$ integrin. *Nature 372:190.*
44. James, S. P., and H. Kiyono. 1999. Gastrointestinal lamina propria T cells. In *Mucosal Immunology.* P. L. Ogra, M. E. Lamm, J. Bienenstock, J. Mestecky, W. Strober, and J. R. McGhee, eds. Academic Press, San Diego, p. 381.
45. Schon, M. P., M. Schon, H. B. Warren, J. P. Donohue, and C. M. Parker. 2000. Cutaneous inflammatory disorder in integrin α_E (CD103)-deficient mice. *J. Immunol. 165:6583.*
46. Ronchetti, S., G. Nocentini, C. Riccardi, and P. P. Pandolfi. 2002. Role of GITR in activation response of T lymphocytes. *Blood 100:350.*

Mucosal T Cells Expressing High Levels of IL-7 Receptor Are Potential Targets for Treatment of Chronic Colitis[1]

Motomi Yamazaki,* Tomoharu Yajima,† Masanobu Tanabe,‡ Kazuto Fukui,† Eriko Okada,* Ryuichi Okamoto,* Shigeru Oshima,* Tetsuya Nakamura,* Takanori Kanai,* Masahiro Uehira,¶ Tsutomu Takeuchi,‡ Hiromichi Ishikawa,§ Toshifumi Hibi,† and Mamoru Watanabe[2]*

The IL-7/IL-7R-dependent signaling pathway plays a crucial role in regulating the immune response in intestinal mucosa. Here we demonstrate the pivotal role of this pathway in the development and treatment of chronic colitis. T cells expressing high levels of IL-7R were substantially infiltrated in the chronic inflamed mucosa of TCR α-chain knockout mice and IL-7 transgenic mice. Transfer of mucosal T cells expressing high levels of IL-7R, but not T cells expressing low levels of IL-7R, from these mice into recombinase-activating gene-2$^{-/-}$ mice induced chronic colitis. Selective elimination of T cells expressing high levels of IL-7R by administrating small amounts of toxin-conjugated anti-IL-7R Ab completely ameliorated established, ongoing colitis. These findings provide evidence that therapeutic approaches targeting mucosal T cells expressing high levels of IL-7R are effective in the treatment of chronic intestinal inflammation and may be feasible for use in the therapy of human inflammatory bowel disease. ***The Journal of Immunology,*** **2003, 171: 1556–1563.**

Interleukin-7 is a nonredundant cytokine for the development of lymphocyte lineage cells (1). Abundant IL-7 expression has been demonstrated in the bone marrow stroma, thymus, spleen, and liver. However, a potential role for IL-7 in peripheral nonlymphoid tissues remained unclear. We have demonstrated that IL-7 is produced by intestinal epithelial cells and regulates mucosal lymphocytes (2). Following our study, other investigators demonstrated that IL-7 is crucial for the development of TCR-$\gamma\delta$ T cells and the formation of Peyer's patches in the intestinal mucosa of the mouse (3–6). TCR-$\gamma\delta$ intraepithelial lymphocytes (IELs)[3] are completely absent from IL-7R knockout mice, and their number is extremely decreased in IL-7 knockout mice. It has been demonstrated that IL-7 expression under intestinal fatty acid binding protein promoter in intestinal epithelial cells of IL-7 knockout mice was sufficient for the development of extrathymic TCR-$\gamma\delta$ IELs (7). The effect of IL-7 expression on the development of Peyer's patches further emphasized the critical role for IL-7 in the ontogeny of the mucosal immune system. Moreover, we have recently demonstrated the presence of a novel lymphoid tissue, designated cryptopatches, in murine intestinal mucosa, where clusters of IL-7R$^+$c-Kit$^+$ lympho-hemopoietic progenitor develop in an IL-7-dependent fashion (8, 9). All these findings indicated that intestinal epithelial cell-derived IL-7 plays a crucial role in the organization of mucosal lymphoid tissues and in the regulation of the normal immune response in the intestinal mucosa.

However, the role of IL-7/IL-7R-dependent signals during inflammation and in human intestinal disease is poorly understood. We tried to clarify the mechanism by which locally produced IL-7 regulates mucosal lymphocytes and the role of mucosal IL-7/IL-7R-dependent signals in chronic intestinal inflammation. We have demonstrated that mucosal IL-7/IL-7R-mediated immune responses are dysregulated at the chronic inflammation sites in human ulcerative colitis (our unpublished observation). We have also demonstrated that IL-7 transgenic (Tg) mice developed chronic colitis (10, 11). IL-7 Tg mice frequently showed rectal prolapse and remittent intestinal bleeding at 8–12 wk of age. Histopathological examination of the colonic tissues revealed the development of chronic colitis that mimicked histopathological characteristics of ulcerative colitis in humans. Of note, IL-7 protein accumulation was significantly decreased in the epithelial cells of the inflamed region of chronic colitis, both in human ulcerative colitis and in the colitis region of IL-7 Tg mice. IL-7R$^+$ cells were significantly infiltrated in the lamina propria at the colitis lesions. These findings in human ulcerative colitis and IL-7 Tg mice indicated that chronic inflammation of the colonic mucosa may be mediated by dysregulation or down-regulation of epithelial cell-derived IL-7 and by infiltration of IL-7R$^+$ T cells in both human and rodents.

Here we demonstrate the essential role of the mucosal IL-7R-dependent pathway in the development of chronic intestinal inflammation. We provide evidence that infiltration of highly IL-7R α-chain-expressing T cells is a common characteristic of chronic colitis, and new therapeutic approaches targeting mucosal T cells expressing high levels of IL-7R were successful in the treatment of chronic intestinal inflammation in mouse models without deletion

*Department of Gastroenterology and Hepatology, Graduate School, Tokyo Medical and Dental University, Tokyo, Japan; Departments of †Internal Medicine, ‡Tropical Medicine and Parasitology, and §Microbiology, Keio University School of Medicine, Tokyo, Japan; and ¶Shionogi Research Laboratories, Osaka, Japan

Received for publication February 24, 2003. Accepted for publication May 27, 2003.

The costs of publication of this article were defrayed in part by the payment of page charges. This article must therefore be hereby marked *advertisement* in accordance with 18 U.S.C. Section 1734 solely to indicate this fact.

[1] This work was supported in part by Grants-in-Aid for Scientific Research from Scientific Research on Priority Areas, Exploratory Research, and Creative Scientific Research from the Japanese Ministry of Education, Culture, Sports, Science, and Technology; the Japanese Ministry of Health, Labor, and Welfare; the Foundation for Advancement of International Science; the Terumo Lifescience Foundation; and the Ohyama Health Foundation.

[2] Address correspondence and reprint requests to Dr. Mamoru Watanabe, Department of Gastroenterology and Hepatology, Graduate School, Tokyo Medical and Dental University, 1-5-45 Yushima, Bunkyo-ku, Tokyo 113-8519, Japan. E-mail address: mamoru.gast@tmd.ac.jp

[3] Abbreviations used in this paper: IEL, intraepithelial lymphocyte; DSS, dextran sulfate sodium; LPL, lamina propria lymphocyte; RAG, recombinase-activating gene; Tg, transgenic.

0022-1767/03/$02.00

of cells with low or intermediate expression of IL-7R. We have shown that the mucosal IL-7R-dependent signaling pathway in the colonic mucosa was dysregulated in human ulcerative colitis. Therefore, our results indicated the potential of targeting mucosal T cells expressing high levels of IL-7R for the therapy of human inflammatory bowel disease.

Materials and Methods

Mice

TCR α-chain knockout (TCR$\alpha^{-/-}$) mice with a background of C57BL/6 were purchased from The Jackson Laboratory (Bar Harbor, ME). C57BL/6 recombinase-activating gene-2 (RAG-2)$^{-/-}$ mice were provided by Central Laboratories for Experimental Animals (Kawasaki, Japan). BALB/c and C.B.17-SCID mice were purchased from Japan Clea (Tokyo, Japan). IL-7 Tg mice carrying murine IL-7 cDNA under the control of the SRα promoter were established as previously described (10). In some experiments wild-type littermates were used as controls. Mice were maintained at the animal care facility of Tokyo Medical and Dental University. The review board of the university approved our experimental animal studies.

Induction of experimentally induced colitis

For chemically induced colitis, we used dextran sulfate sodium (DSS)-induced, oxazolone-induced, and 2,4,6-trinitrobenzene sulfonic acid (TNBS)-immune colitis models (12). These models developed acute or short term colitis. CD4$^+$CD45RB^{high} T cell transfer model using C.B.17-SCID mice (13) was also used as a chronic colitis model.

Histological and immunohistochemical analyses

Colonic tissues were embedded at −80°C. Six-micrometer sections were placed on glass slides and stained with H&E. The severity of colitis was graded by histological findings. The disease score (0, normal; 1, mild; 2, moderate; 3, severe colitis) in stained sections were determined according to the degree of inflammation as previously described (14). For the staining of IL-7R$^+$ cells, sections were incubated with 10 μg/ml of anti-IL-7R mAb (A7R34, provided by Dr. T. Sudo, Toray Industries, Tokyo, Japan). Isotype-matched control Abs were used as controls. Staining of the sections was performed using the avidin-biotin complex method (Vectastain ABC kit; Vector Laboratories, Burlingame, CA). Staining was then visualized using diaminobenzidine solution, and the slides were then counterstained with hematoxylin.

Preparation of colonic lamina propria lymphocytes (LPLs)

For the isolation of LPLs from colon, nonadherent mesenteric tissues were removed, and the entire colon was opened longitudinally, washed, and cut into pieces. The dissected mucosa was incubated with Ca^{2+}, Mg^{2+}-free HBSS containing 1 mM DTT (Life Technologies, Gaithersburg, MD) for 30 min at 37°C with gentle stirring, and this step was repeated. The residing tissue fragments were washed and incubated with collagenase A (Roche, Mannheim, Germany) for 2 h at 37°C. The supernatants were collected and washed, and the lymphocyte fraction was isolated on discontinuous Percoll gradients of 75 and 40%.

Flow cytometry

The profile of LPLs of the colon was analyzed by flow cytometry. To detect the expression of a variety of molecules on the cell surface, isolated cells were preincubated with a FcγR-blocking mAb (CD16/32; 2.4G2; BD PharMingen, San Diego, CA) for 20 min, followed by incubation with FITC-, PE-, or biotin-labeled specific Abs for 30 min on ice. The mAbs used were anti-CD4 mAb (anti-L3T4, RM4-5; BD PharMingen), TCR-β mAb (H57-597; BD PharMingen), and anti-IL-7R mAb. Biotinylated Abs were detected with PE-streptavidin (BD PharMingen). Standard two-color flow cytometric analysis was performed using FACSCalibur (BD Biosciences, Mountain View, CA) with CellQuest software. Staining with control irrelevant isotype-matched mAbs assessed background fluorescence. Dead cells were eliminated from analysis by propidium iodide staining.

Cytokine-specific ELISA

To measure cytokine production, isolated LPLs were cultured in medium supplemented with 1 μg/ml of soluble anti-CD28 mAb (37.51; BD PharMingen) in 96-well plates precoated with 10 μg/ml of anti-CD3 mAb (145-2C11; BD PharMingen) in PBS. Culture supernatants were collected, and the cytokine concentrations of IL-2, IL-4, IL-10 and IFN-γ were determined by specific ELISA (Endogen, Woburn, MA).

Cell transfer experiments

CD4$^+$ T cells were separated from colonic LPLs from colitis-free TCR$\alpha^{-/-}$ mice (4 wk of age), TCR$\alpha^{-/-}$ mice with chronic colitis (20 wk of age), and IL-7 Tg mice (60 wk of age) by MACS (Miltenyi Biotech, Bergisch Gladbach, Germany). We then sorted IL-7R$^+$ T cells using FACSVantage (BD Biosciences). The purity of IL-7R$^+$ T cells was confirmed by flow cytometry and was >97%. The purified IL-7R$^+$ T cells were i.p. transferred into RAG-2$^{-/-}$ mice (8–10 wk of age). Mice were sacrificed 4–6 wk after cell transfer for analysis. In some experiments purified CD4$^+$IL-7R$^+$ T cells from colitic mice were further separated into cells expressing high and low levels of IL-7R. In the histogram of IL-7R expression determined by flow cytometry, the top 30% of the cells were separated as IL-7R^{high} cells and the bottom 30% of the cells were separated as IL-7R^{low}. We then transferred 5×10^5 of either IL-7R^{high} or IL-7R^{low} mucosal T cells into RAG-2$^{-/-}$ mice.

Administration of saporin-conjugated anti-IL-7R mAb

We conjugated the plant toxin saporin to our anti-IL-7R mAb (A7R34) as a custom service at Advance Targeting System (Carlsbad, CA). We then treated chronic colitis in TCR$\alpha^{-/-}$ mice from 20–24 wk of age by i.p. injection of this toxin-conjugated anti-IL-7R mAb at a dose of 10 μg, once a week for 6 wk. As a control, the same amount of a mixture of free anti-IL-7R mAb (10 μg) and saporin (unconjugated) was injected. All mice were sacrificed on the day after the last treatment, and colitis lesions were evaluated.

Statistical analysis

The results were expressed as the mean ± SD. For statistical analysis, we used the program StatView for Macintosh (Abacus Concepts, Berkley, CA) and MS Office (Excel; Microsoft, Redmond, WA) and analyzed the data with Student's *t* test.

Results

Infiltration of T cells expressing high levels of IL-7R in the colonic mucosa of TCR$\alpha^{-/-}$ mice with chronic colitis

We assessed whether the mucosal IL-7R-dependent immune response is dysregulated in the development of acute and chronic intestinal inflammation. As acute or short term colitis models, we used chemically induced colitis models, including DSS-induced, oxazolone-induced, and TNBS-immune colitis models. As chronic or long term colitis models, CD4$^+$CD45RB^{high} T cell transfer into the SCID mice model and TCR$\alpha^{-/-}$ mice (14) were examined. No changes in IL-7/IL-7R-mediated immune responses were observed in the inflamed colonic mucosa of chemically induced acute colitis models (data not shown). TNBS-treated mice developed short term colitis, but IL-7R$^+$ T cells did not infiltrate the lamina propria of the inflamed mucosa. This was also observed in oxazolone-treated mice and the DSS-induced mouse colitis model. In contrast, IL-7R$^+$ T cells were remarkably infiltrated in lamina propria of chronically inflamed mucosa of CD4$^+$CD45RB^{high} T cell-transferred SCID mice. These results are consistent with the findings in IL-7 Tg mice and in human ulcerative colitis. The results suggested that mucosal IL-7R-dependent immune responses were involved in chronic intestinal inflammation, but not in acute inflammation.

To prove this possibility, we then focused on TCR$\alpha^{-/-}$ mice. Our TCR$\alpha^{-/-}$ mice spontaneously developed chronic colitis at 8–16 wk of age (14). We assessed the expression of IL-7R on infiltrated mucosal T cells before and after the development of colitis. In TCR$\alpha^{-/-}$ mice, previous reports showed that CD4$^+$TCRβ^{dim} T cells mediate chronic colitis (15, 16). Flow cytometric analysis of isolated LPLs demonstrated that CD4$^+$ TCRβ^{dim} T cells were demonstrable in the colonic mucosa of both colitis-free TCR$\alpha^{-/-}$ mice and mice with chronic colitis. However, IL-7R$^+$TCRβ^{dim} T cells were remarkably increased in colonic LPLs after the development of colitis (Fig. 1*A*). In the colonic mucosa of colitis-free TCR$\alpha^{-/-}$ mice, TCRβ^{dim} LPLs were demonstrable, but only half of these cells expressed IL-7R. In contrast, almost all TCRβ^{dim} cells in the colonic mucosa of TCR$\alpha^{-/-}$

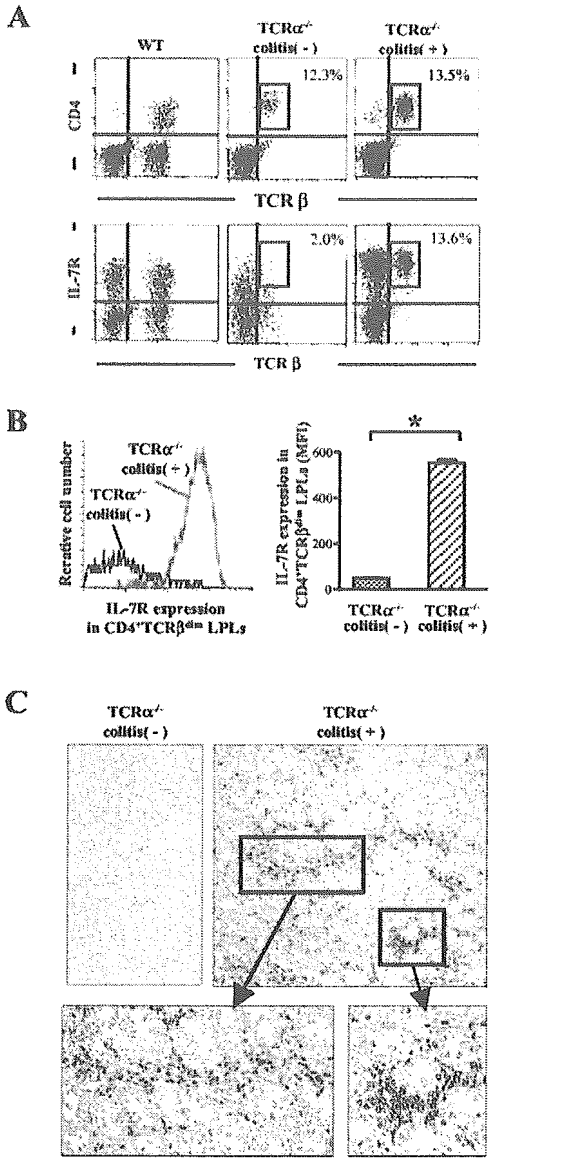

FIGURE 1. Infiltration of LPLs expressing IL-7R at a high level in the colonic mucosa of TCR$\alpha^{-/-}$ mice with chronic colitis. *A*, Flow cytometric analysis of isolated LPLs demonstrated that CD4$^+$TCRβ^{dim} T cells were demonstrable in the colonic mucosa of both colitis-free TCR$\alpha^{-/-}$ mice (n = 18) and TCR$\alpha^{-/-}$ mice with chronic colitis (n = 28), but not in that of wild-type littermates (WT; n = 32). However, IL-7R$^+$TCRβ^{dim} T cells were remarkably increased in colonic LPLs after the development of colitis. In the colonic mucosa of colitis-free TCR$\alpha^{-/-}$ mice, TCRβ^{dim} LPLs were demonstrable, but only half these cells expressed IL-7R. In contrast, almost all TCRβ^{dim} T cells in the colonic mucosa of TCR$\alpha^{-/-}$ mice with chronic colitis expressed IL-7R. *B*, The degree of IL-7R expression in CD4$^+$TCRβ^{dim} LPLs in the colonic mucosa of TCR$\alpha^{-/-}$ mice with chronic colitis (n = 28) was significantly (*, $p < 0.001$) higher than that in the colonic mucosa of colitis-free TCR$\alpha^{-/-}$ mice (n = 18; mean fluorescence intensity (MFI), 553 ± 21 and 41 ± 5, respectively). *C*, There were only a few IL-7R$^+$ cells in the colonic mucosa of colitis-free TCR$\alpha^{-/-}$ mice (n = 10) or wild-type mice (n = 21). In contrast, cells expressing IL-7R at a high level detected by immunohistochemistry were predominantly infiltrated in the lamina propria at chronic colitis lesions in TCR$\alpha^{-/-}$ mice (n = 20). These data are representative of four separate series of experiments.

mice with chronic colitis expressed IL-7R. Moreover, the degree of IL-7R expression in CD4$^+$TCRβ^{dim} LPLs of the colonic mucosa of TCR$\alpha^{-/-}$ mice with chronic colitis was significantly ($p <$ 0.001) higher compared with that in the colonic mucosa of colitis-free TCR$\alpha^{-/-}$ mice (Fig. 1*B*). The degrees of IL-7R expression determined by the mean fluorescence intensity in flow cytometric histogram were 553 ± 21 and 41 ± 5, respectively. To confirm that infiltrated CD4$^+$ T cells expressed IL-7R at high level in the chronic inflamed colonic mucosa, we then performed immunohistochemistry. There were only a few IL-7R$^+$ cells in the colonic mucosa of colitis-free TCR$\alpha^{-/-}$ mice or wild-type mice. In contrast, T cells expressing intense staining signals of IL-7R were predominantly infiltrated in the lamina propria at chronic colitis lesions in TCR$\alpha^{-/-}$ mice (Fig. 1*C*). Most of these infiltrated cells expressed CD4. In addition, IL-7R transcript was up-regulated in chronic colitis lesions, as determined by RT-PCR (data not shown). These results further reinforce the concept that IL-7R-mediated immune responses are dysregulated in chronic intestinal inflammation. The expansion of LPLs expressing high levels of IL-7R in the colonic mucosa was a characteristic feature of the chronic colitis lesion.

Transfer of IL-7R^{high} mucosal T cells induced chronic colitis in immunodeficient mice

To prove the hypothesis that T cells expressing high levels of IL-7R in the lamina propria of the colonic mucosa mediated the development of chronic intestinal inflammation, we first performed transfer experiments of mucosal T cells expressing IL-7R into immunodeficient mice. IL-7R$^+$CD4$^+$ T cells were isolated from the colonic mucosa of TCR$\alpha^{-/-}$ mice that developed chronic colitis or wild-type mice by sorting and then were transferred into syngeneic RAG-2$^{-/-}$ mice (Fig. 2*A*). Phenotypic analysis of IL-7R$^+$CD4$^+$ LPLs from TCR$\alpha^{-/-}$ mice with chronic colitis revealed that these isolated cells consisted of 80% TCRβ^{dim} and 20% γδ, 95% CD45RB^{low} and 5% CD45RB^{high}, and CD25$^-$ cells (Fig. 2*B*). Cytokine production of isolated IL-7R$^+$CD4$^+$ LPLs in TCR$\alpha^{-/-}$ mice with chronic colitis and that in wild-type mice after stimulation with anti-CD3 mAb and anti-CD28 mAb were quite different. Isolated IL-7R$^+$CD4$^+$ LPLs from TCR$\alpha^{-/-}$ mice with chronic colitis produced significantly higher amounts of IL-2 ($p < 0.001$), IFN-γ ($p < 0.05$), and IL-4 ($p < 0.01$) compared with those from wild-type mice (Fig. 2*C*). IL-10 production was decreased in isolated IL-7R$^+$CD4$^+$ LPLs from TCR$\alpha^{-/-}$ mice with chronic colitis ($p < 0.05$ compared with that from wild-type mice).

All recipient mice transferred 5 × 10^5 IL-7R$^+$CD4$^+$ LPLs from TCR$\alpha^{-/-}$ mice with chronic colitis developed severe colitis within 4–6 wk (Fig. 2*D*). Colonic inflammation occurred more rapidly and was more severe in the recipient mice compared with the original TCR$\alpha^{-/-}$ mice. Histopathological examination of the colonic tissues revealed that inflammatory cell infiltration and goblet cell depletion were prominent throughout the colon. Crypt abscesses, Paneth cell metaplasia, and infiltration of eosinophils were also observed in the inflammatory lesions. These features resembled the histopathological characteristics of the colitic lesion of TCR$\alpha^{-/-}$ mice and our IL-7 Tg mice (10, 14–16). In contrast, transfer of IL-7R$^+$CD4$^+$ LPLs from wild-type mice into RAG-2$^{-/-}$ mice did not produce colitis in the mice during the observation period. In addition, IL-7R$^-$CD4$^+$ LPLs from both mice never induced colitis. In the chronic colitis lesion of RAG-2$^{-/-}$ mice transferred IL-7R$^+$CD4$^+$ LPLs from TCR$\alpha^{-/-}$ mice with chronic colitis, IL-7R$^+$ T cells were remarkably infiltrated in the lamina propria (Fig. 2*D*). Flow cytometric analysis revealed that these infiltrated LPLs mainly consisted of TCRβ^{dim}, CD4$^+$, CD4$^+$CD45RB^{low}, and CD25$^-$ cells (Fig. 2*E*).

To eliminate the possibility that not mucosal T cells expressing high levels of IL-7R, but merely CD4$^+$TCRβ^{dim} T cells mediated

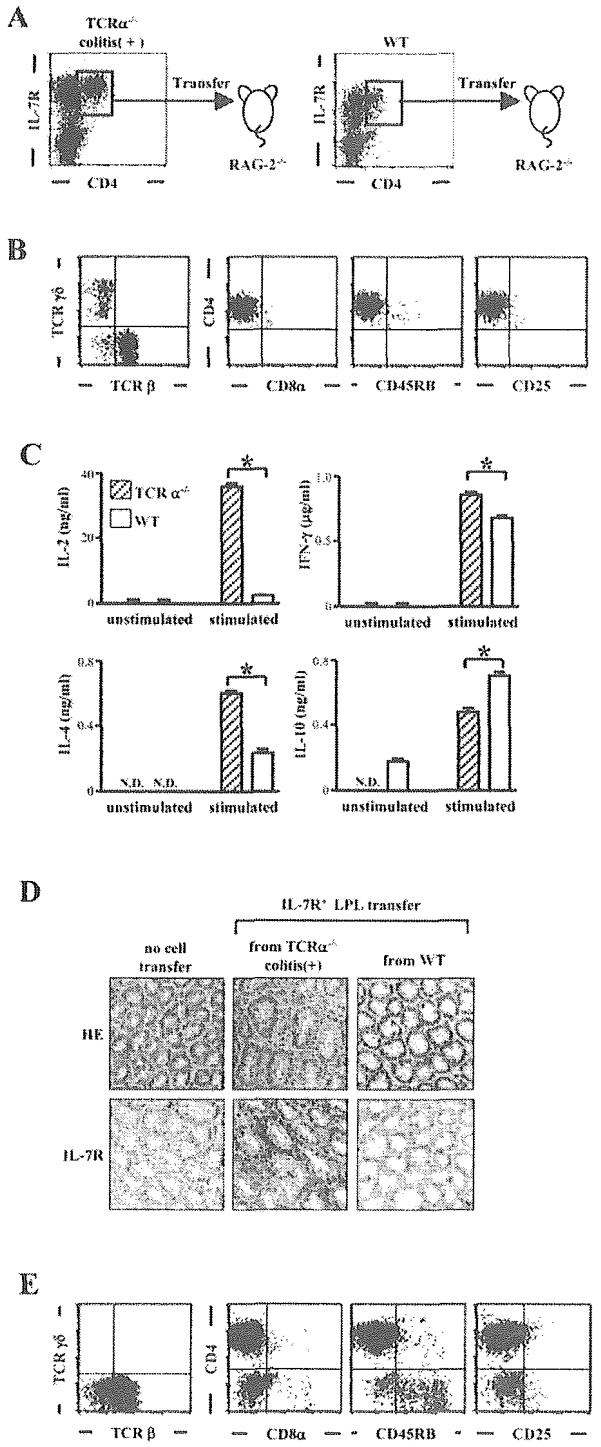

FIGURE 2. Transfer of IL-7R$^+$CD4$^+$ LPLs from TCR$\alpha^{-/-}$ mice into RAG-2$^{-/-}$ mice induced chronic colitis. *A*, IL-7R$^+$CD4$^+$ T cells were isolated from the colonic mucosa of both TCR$\alpha^{-/-}$ mice with chronic colitis and wild-type mice by sorting and then were transferred into syngeneic RAG-2$^{-/-}$ mice. *B*, Phenotypic analysis of IL-7R$^+$CD4$^+$ LPLs from TCR$\alpha^{-/-}$ mice with chronic colitis (n = 10) revealed that these isolated cells consisted of 80% TCRβ^{dim} and 20% γδ, 95% CD45RB^{low} and 5% CD45RB^{high}, and CD25$^-$ cells. *C*, Cytokine production of isolated IL-7R$^+$CD4$^+$ LPLs from TCR$\alpha^{-/-}$ mice with chronic colitis (n = 8) and wild-type mice (n = 10) after stimulation with anti-CD3 mAb and anti-CD28 mAb presented remarkable differences. Isolated IL-7R$^+$CD4$^+$ LPLs from TCR$\alpha^{-/-}$ mice with chronic colitis produced significantly higher amounts of IL-2 (*, $p < 0.001$), IFN-γ (*, $p < 0.05$), and IL-4 (*, $p < 0.01$) compared with those from wild-type mice. IL-10 production was decreased in isolated IL-7R$^+$CD4$^+$ LPLs from TCR$\alpha^{-/-}$ mice with chronic colitis (*, $p < 0.05$ compared with that from wild-type mice). *D*, All the recipient RAG-2$^{-/-}$ mice that were transferred 5 × 10^5 IL-7R$^+$CD4$^+$ LPLs/body from TCR$\alpha^{-/-}$ mice with chronic colitis developed severe colitis at 4–6 wk after transfer (n = 30). Colonic inflammation occurred at earlier periods and more severely in these mice than in the original TCR$\alpha^{-/-}$ mice. Histopathological examination of the colonic tissues revealed that inflammatory cell infiltration and goblet cell depletion were most prominent throughout the colon. In contrast, transfer of the same numbers of IL-7R$^+$CD4$^+$ LPLs from wild-type mice into RAG-2$^{-/-}$ mice did not produce colitis during the observation period (n = 10). In chronic colitis lesion of RAG-2$^{-/-}$ mice transferred CD4$^+$IL-7R$^+$ LPLs from TCR$\alpha^{-/-}$ mice with chronic colitis, IL-7R$^+$ T cells were remarkably infiltrated in the lamina propria. In the colonic mucosa of RAG-2$^{-/-}$ mice that were transferred IL-7R$^+$ LPLs from wild-type mice, IL-7R$^+$ T cells were not infiltrated in the lamina propria. These data are representative of four separate series of experiments. *E*, Flow cytometric analysis revealed that infiltrated IL-7R$^+$ LPLs mainly consisted of TCRβ^{dim}, CD4$^+$, CD4$^+$CD45RB^{low}, and CD25$^-$ cells in the chronic colitis lesion of RAG-2$^{-/-}$ mice that were transferred IL-7R$^+$CD4$^+$ LPLs from TCR$\alpha^{-/-}$ mice with chronic colitis (n = 8).

chronic inflammation, we performed another set of transfer experiments using purified and sorted IL-7R$^+$CD4$^+$ T cells from the mucosa of TCR$\alpha^{-/-}$ mice with chronic colitis. Purified IL-7R$^+$CD4$^+$ LPLs from TCR$\alpha^{-/-}$ mice with chronic colitis were further separated into cells expressing IL-7R at high and low levels. In the flow cytometric histogram of IL-7R expression, the highest 30% of IL-7R-expressing T cells were separated as IL-7R^{high} cells, and the lowest 30% of IL-7R expressing T cells were separated as IL-7R^{low} cells (Fig. 3*A*). We transferred 5 × 10^5 cells/body of those sorted cells into RAG-2$^{-/-}$ mice. All recipient RAG-2$^{-/-}$ mice that were transferred IL-7R^{high} LPLs developed severe colitis within 4–6 wk after transfer (Fig. 3*B*). In sharp contrast, none of mice that were transferred IL-7R^{low} LPLs developed colitis during the observation period. Assessment of the severity of colitis examined by histological scores showed a significant ($p < 0.001$) difference between mice transferred IL-7R^{high} LPLs and those given IL-7R^{low} LPLs (Fig. 3*C*). These results supported the concept that IL-7R^{high} T cells, not merely CD4$^+$TCRβ^{dim} T cells, in lamina propria of colonic mucosa induced chronic colitis.

To further eliminate the possibility that not IL-7R^{high} mucosal T cell, but TCRβ^{dim} T cells mediated chronic inflammation, we performed another transfer experiment using IL-7R$^+$ T cells from IL-7 Tg mice. In IL-7 Tg mice, purified IL-7R$^+$ T cells from colitic lesions of IL-7 Tg mice contained no TCRβ^{dim} T cells (Fig. 4*A*). We also sorted IL-7R^{high} and IL-7R^{low} CD4$^+$ T cells from the colonic mucosa of IL-7 Tg mice that developed chronic colitis and transferred these sorted cells as well as whole IL-7R$^+$ T cells into RAG-2$^{-/-}$ mice (Fig. 4*B*). All recipient mice that were transferred IL-7R^{high} mucosal T cells or whole IL-7R$^+$ T cells from IL-7 Tg mice developed severe colitis within 4 wk (Fig. 4*C*). In contrast, transfer of IL-7R^{low} T cells did not induce inflammation. Similar to the transfer experiments with IL-7R^{high} mucosal T cells from TCR$\alpha^{-/-}$ mice, colonic inflammation occurred more rapidly and was more severe in the recipient mice compared with the colitis in original IL-7 Tg mice. Histopathological examination of the colonic tissues of those transferred mice revealed that inflammatory cell infiltration and goblet cell depletion were most prominent throughout the colon. Crypt abscesses, Paneth cell metaplasia, and infiltration of eosinophils were also observed in the colitis lesions. Assessment of the severity of colitis by histological scores showed a significant ($p < 0.001$) difference between mice transferred IL-7R^{high} LPLs and those given IL-7R^{low} from the colitic lesion of IL-7 Tg mice (Fig. 4*D*). All these results indicated that mucosal T cells expressing high levels of IL-7R mediated the development of

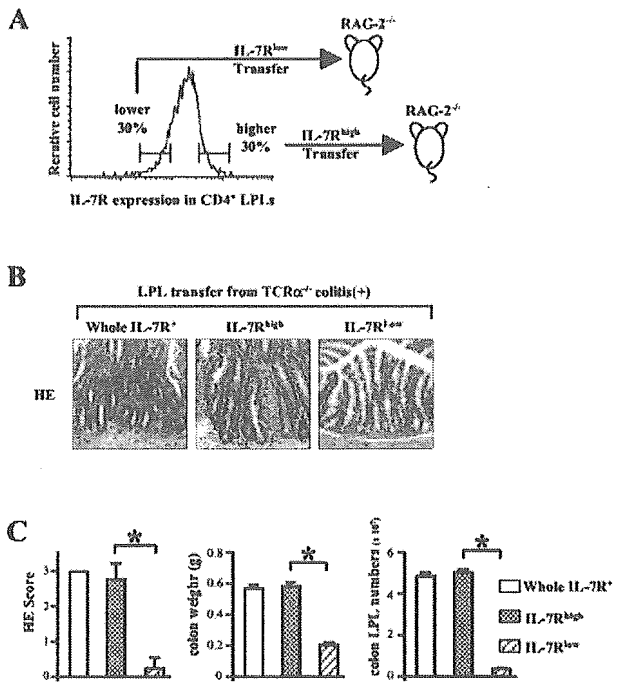

FIGURE 3. Transfer of LPLs expressing IL-7R at a high level from TCR$\alpha^{-/-}$ mice into RAG-2$^{-/-}$ mice induced chronic colitis. *A*, Purified IL-7R^{+}CD4^{+} LPLs from TCR$\alpha^{-/-}$ mice with chronic colitis were further separated into cells expressing IL-7R at high and low levels. In the flow cytometric histogram of IL-7R expression, the top 30% of IL-7R-expressing T cells were separated as IL-7R^{high} cells, and the bottom 30% of IL-7R expressing T cells were separated as IL-7R^{low} cells. We transferred 5×10^5 cells/body of those sorted cells into RAG-2$^{-/-}$ mice. *B*, All recipient RAG-2$^{-/-}$ mice that were transferred IL-7R^{high} LPLs ($n = 12$) developed severe colitis within 4–6 wk. In sharp contrast, none of mice that were transferred IL-7R^{low} LPLs from same mice ($n = 9$) developed colitis during the observation period. *C*, Assessment of the severity of the colitis by histological scores showed a significant (*, $p < 0.001$) difference between the recipient mice transferred IL-7R^{high} LPLs and those given IL-7R^{low}. These data are representative of three separate series of experiments.

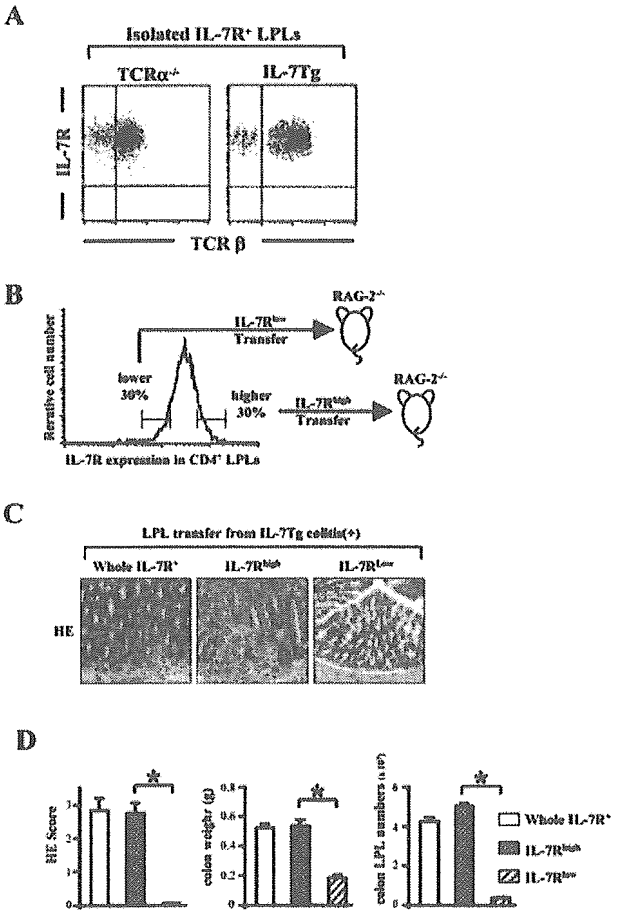

FIGURE 4. Transfer of sorted IL-7R^{high} LPLs from IL-7 Tg mice into RAG-2$^{-/-}$ mice induced chronic colitis. *A*, Purified CD4^{+} LPLs from the colonic mucosa of IL-7 Tg mice with chronic colitis contained no TCRβ^{dim} T cells. *B*, We sorted IL-7R^{high} and IL-7R^{low} CD4^{+} T cells from the colonic mucosa of IL-7 Tg mice with chronic colitis as described in Fig. 3 and transferred these sorted as well as unfractionated IL-7R^{+} T cells into RAG-2$^{-/-}$ mice. *C*, All recipient mice that were transferred IL-7R^{high} mucosal T cells ($n = 12$) as well as unfractionated IL-7R^{+} T cells from IL-7 Tg mice ($n = 8$) developed severe colitis within 4 wk after cell transfer. In contrast, transfer of IL-7R^{low} T cells did not induce inflammation ($n = 8$). Similar to TCR$\alpha^{-/-}$ IL-7R^{high} mucosal T cell transfer experiments, colonic inflammation occurred more rapidly and was more severe in the recipient mice compared with that in the original IL-7 Tg mice. Histopathological examination of the colonic tissues revealed that inflammatory cell infiltration and goblet cell depletion were prominent throughout the colon. *D*, Assessment of the severity of colitis by histological scores showed a significant (*, $p < 0.001$) difference between the recipient mice that were transferred either IL-7R^{high} LPLs or IL-7R^{low} and the colitic IL-7 Tg mice. These data are representative of three separate series of experiments.

chronic intestinal inflammation. Therefore, therapeutic approaches targeting IL-7R-mediated immune responses are thought to be feasible.

Successful treatment of established, ongoing chronic colitis in TCR$\alpha^{-/-}$ mice by selective elimination of LPLs expressing high levels of IL-7R using saporin-conjugated anti-IL-7R Ab

To correct the dysregulation of mucosal IL-7/IL-7R-mediated immune responses, we attempted to control mucosal T cells expressing high levels of IL-7R. On the basis of previous findings, we then tried to eliminate mucosal T cells expressing high levels of IL-7R by toxin-based destruction of IL-7R-expressing cells. A plant toxin, saporin, was conjugated to our anti-IL-7R mAb (17). In preliminary experiments we confirmed that a low concentration (10 μg/ml) of saporin-conjugated anti-IL-7R mAb inhibited the proliferation of IL-7-dependent cell line DW34 cells expressing IL-7R at a high level, but not of LPLs and spleen cells from wild-type mice. Using 10 μg/ml of this toxin-conjugated anti-IL-7R mAb, we found that this agent did not inhibit the in vitro proliferation of CD4^{+} spleen cells that expressed IL-7R at low and intermediate levels from wild-type mice, but did inhibit that of IL-7R^{high} T cells from chronically inflamed mucosa of TCR$\alpha^{-/-}$ mice (data not shown). In preliminary experiments treatment of wild-type mice by i.p. injection of small amounts (10 μg/body) of saporin-conjugated anti-IL-7R mAb once a week for 6 wk did not cause any change in the total cell number and phenotypic change in spleen cells or LPLs (data not shown). Depletion of IL-7R^{+} or CD4^{+} cells was not observed even after six treatments with 10 μg/body of saporin-conjugated anti-IL-7R mAb. We then assessed the therapeutic effect of this saporin-conjugated anti-IL-7R mAb in the established, ongoing colitis of TCR$\alpha^{-/-}$ mice. Since all untreated TCR$\alpha^{-/-}$ mice developed colitis within 16 wk of age in our series, we started the treatment of established colitis in these mice at 20 wk of age. We treated chronic colitis in TCR$\alpha^{-/-}$ mice by i.p. injection of small amounts (10 μg/body) of saporin-conjugated anti-IL-7R mAb, once a week for 6 wk. Selective elimination of IL-7R^{high} LPLs by the administration of small amounts of

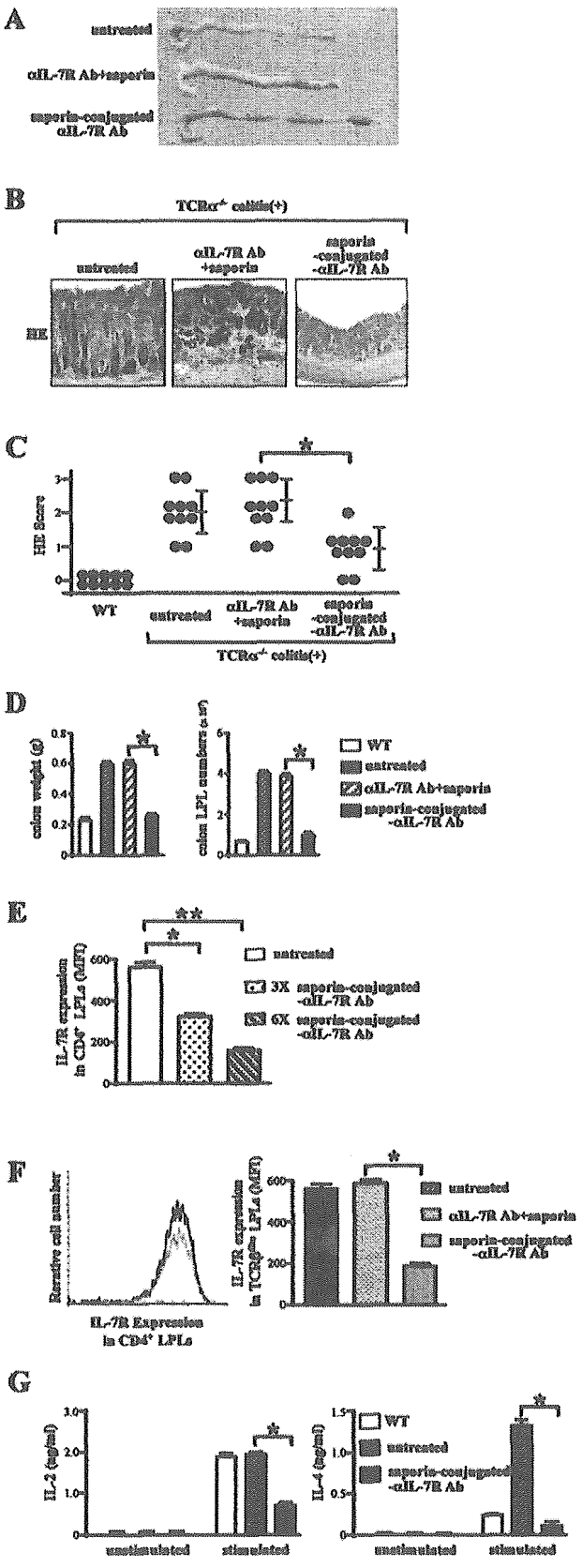

FIGURE 5. Successful treatment of established, ongoing chronic colitis in TCR$\alpha^{-/-}$ mice by the selective elimination of LPLs expressing IL-7R at a high level using saporin-conjugated anti-IL-7R Ab. All untreated TCR$\alpha^{-/-}$ mice developed colitis within 16 wk of age in our series; therefore, we started the treatment of this established, ongoing colitis in these mice at 20 wk of age. We treated chronic colitis in the TCR$\alpha^{-/-}$ mice by i.p. injection of small amounts (10 μg/body) of saporin-conjugated anti-IL-7R mAb, once a week for 6 wk. *A*, Gross inspection of the colon in TCR$\alpha^{-/-}$ mice revealed a complete reduction in the inflammatory activity after treatment with saporin-conjugated anti-IL-7R mAb (n = 16), comparable to the colitis observed in wild-type mice (n = 20). In contrast, TCR$\alpha^{-/-}$ mice treated with a mixture of free anti-IL-7R mAb and saporin (not conjugated) using the same protocol (n = 14) developed severe colitis, comparable to that in untreated TCR$\alpha^{-/-}$ mice. *B*, Histological analysis of saporin-conjugated anti-IL-7R mAb-treated mice showed the dramatic decrease in colonic inflammation, comparable to the histology of the colonic mucosa in wild-type mice. In contrast, TCR$\alpha^{-/-}$ mice treated with a mixture of free anti-IL-7R mAb and saporin developed severe colitis. *C*, The histological score was significantly (*, $p < 0.01$) decreased after saporin-conjugated anti-IL-7R mAb treatment (n = 10) compared with that after treatment with a mixture of free anti-IL-7R mAb and saporin (n = 10). *D*, The colonic wet weight and isolated cell number of colonic LPLs were significantly (*, $p < 0.001$) decreased in TCR$\alpha^{-/-}$ mice after saporin-conjugated anti-IL-7R mAb treatment (n = 16) compared with those after treatment with a mixture of free anti-IL-7R mAb and saporin (n = 14). The decrease reached the level in wild-type mice. *E*, Flow cytometric analysis of isolated LPLs revealed that the degree of IL-7R expression on CD4$^+$ LPLs from the colonic mucosa of TCR$\alpha^{-/-}$ mice with chronic colitis was gradually and significantly (*, $p < 0.01$; **, $p < 0.001$) decreased after saporin-conjugated anti-IL-7R mAb treatment. The decrease in IL-7R expression was more prominent after six treatments (6X; n = 16) than that after three treatments (3X; n = 5). *F*, Saporin-conjugated anti-IL-7R mAb treatment induced a significant (*, $p < 0.001$) decrease in IL-7R expression on CD4$^+$ LPLs in the colonic mucosa of TCR$\alpha^{-/-}$ mice with chronic colitis (n = 16) compared with that after treatment with a mixture of free anti-IL-7R mAb and saporin (n = 14). The degree of IL-7R expression in CD4$^+$ LPLs after treatment with a mixture of free anti-IL-7R mAb and saporin was comparable to that in untreated TCR$\alpha^{-/-}$ mice (n = 20). *G*, Saporin-conjugated anti-IL-7R mAb treatment induced a significant (*, $p < 0.001$) reduction in IL-2 production by CD4$^+$ mucosal T cells after stimulation with anti-CD3 and anti-CD28 mAbs. IL-4 production increased in CD4$^+$ LPLs from untreated TCR$\alpha^{-/-}$ mice after the same stimulation. This increase was significantly (*, $p < 0.001$) reduced in CD4$^+$ LPLs from saporin-conjugated anti-IL-7R mAb-treated TCR$\alpha^{-/-}$ mice, and production was below the level in wild-type mice. These data are representative of five separate series of experiments.

saporin-conjugated anti-IL-7R mAb completely ameliorated established colitis in TCR$\alpha^{-/-}$ mice. Gross inspection of the colon in TCR$\alpha^{-/-}$ mice revealed complete reduction of inflammatory activity after treatment with saporin-conjugated anti-IL-7R mAb, comparable with that in wild-type mice. In contrast, TCR$\alpha^{-/-}$ mice treated with a mixture of free anti-IL-7R mAb and saporin (not conjugated) using the same protocol developed severe colitis, comparable with that in untreated TCR$\alpha^{-/-}$ mice (Fig. 5*A*). Histological analysis of saporin-conjugated anti-IL-7R mAb-treated mice showed the dramatic decrease in colonic inflammation, comparable with the histology of the colonic mucosa in wild-type mice. In contrast, TCR$\alpha^{-/-}$ mice treated with a mixture of free anti-IL-7R mAb and saporin developed severe colitis (Fig. 5*B*). The histological score assessing the severity of inflammation was significantly ($p < 0.01$) decreased after saporin-conjugated anti-IL-7R mAb treatment compared with that after treatment with a mixture of free anti-IL-7R mAb and saporin (Fig. 5*C*). Colonic wet weight and isolated total cell number of colonic LPLs were significantly ($p < 0.001$) decreased in TCR$\alpha^{-/-}$ mice after saporin-conjugated anti-IL-7R mAb treatment compared with those after treatment with a mixture of free anti-IL-7R mAb and saporin (Fig. 5*D*). The decrease in colonic weight and total LPL number reached the level in wild-type mice. Flow cytometric analysis of isolated LPLs revealed that the degree of IL-7R expression on CD4$^+$ LPLs from the colonic mucosa of TCR$\alpha^{-/-}$ mice with chronic colitis was gradually and significantly ($p < 0.01$) decreased after saporin-conjugated anti-IL-7R mAb treatment (Fig. 5*E*). The decrease in

IL-7R expression was more prominent after six treatments than after three treatments. Subsequently, saporin-conjugated anti-IL-7R mAb treatment induced a significant ($p < 0.001$) decrease in IL-7R expression on $CD4^+$ LPLs in the colonic mucosa of $TCR\alpha^{-/-}$ mice with chronic colitis compared with that after treatment with a mixture of free anti-IL-7R mAb and saporin (Fig. 5*F*). The degree of IL-7R expression in $CD4^+$ LPLs after treatment with a mixture of free anti-IL-7R mAb and saporin was comparable to that in untreated $TCR\alpha^{-/-}$ mice. Saporin-conjugated anti-IL-7R mAb treatment induced a significant ($p < 0.001$) reduction in IL-2 production by $CD4^+$ LPLs after stimulation with anti-CD3 and anti-CD28 mAbs (Fig. 5*G*). IL-4 production was increased in $CD4^+$ LPLs from untreated $TCR\alpha^{-/-}$ mice after stimulation, and this increase was significantly ($p < 0.001$) reduced to the level in wild-type mice in saporin-conjugated anti-IL-7R mAb-treated $TCR\alpha^{-/-}$ mice. These results indicate that successful treatment of established, ongoing chronic colitis was achieved by the selective elimination of LPLs expressing IL-7R at a high level without deletion of cells expressing with low or intermediate levels of IL-7R.

Discussion

A potential role for IL-7/IL-7R-mediated immune responses in the intestinal inflammation was unclear. We have demonstrated that IL-7 Tg mice developed chronic colitis that mimicked histopathological characteristics of human ulcerative colitis. In the colonic mucosa of IL-7 Tg mice with chronic colitis, a decrease in IL-7 protein accumulation in the epithelial cells and marked infiltration of $IL\text{-}7R^+$ T cells in the lamina propria were demonstrable (10, 11). We also showed the decrease in IL-7 protein accumulation in the epithelial cells and infiltration of $IL\text{-}7R^+$ T cells in the lamina propria at the chronic inflammation sites of patients with ulcerative colitis (our unpublished observations). These findings suggest that dysregulation of the mucosal IL-7/IL-7R system is a common phenomenon in chronic inflammation sites of the colonic mucosa. In the present study we confirmed this concept in various chronic colitis mice models. Interestingly, dysregulation of the mucosal IL-7/IL-7R system is not apparent in the acute colitis mouse model. This was consistent with our previous findings. In fact, IL-7 Tg mice developed acute colitis with infiltrating neutrophils and T cells at 1–3 wk of age. In the acute colitis stage, IL-7 protein expression was significantly increased in the inflamed colonic mucosa. This contrasted with the decreased IL-7 expression in the chronic colitis stage, but was consistent with the findings that IL-7 expression was increased in colonic mucosa of patients with acute *Salmonella* enterocolitis and in severely inflamed mucosa in ulcerative colitis at acute exacerbation (our unpublished observations). The reason for substantial proliferation of mucosal $IL\text{-}7R^+$ T cells in chronic colitis, although IL-7 expression in the epithelial cells is decreased, remains unclear. Recent reports indicated that the serum concentration of IL-7 is strongly related to $CD4^+$ T cell lymphopenia, and IL-7 is produced by dendritic-like cells within peripheral lymphoid tissues in HIV disease (18). We are currently investigating the extraintestinal source of IL-7 in murine colitis models.

The most important finding of the present study was that attempts could be feasible in the treatment of chronic intestinal inflammation by the regulation of a mucosal IL-7R-dependent signaling pathway. Increasing evidence showed that chronic colitis in murine models has been successfully prevented by the administration of various mAbs or cytokines and by the establishment of double-knockout mice (19–21). However, few attempts resulted in adequate treatment of the established, ongoing colitis. We prevented chronic colitis in $TCR\alpha^{-/-}$ mice by establishment of $TCR\alpha^{-/-} \times IL\text{-}7R^{-/-}$ double-knockout mice (our unpublished observation). Moreover, we successfully treated established, ongoing colitis in $TCR\alpha^{-/-}$ mice with Ab-based therapy targeting the IL-7R-dependent signaling pathway. We treated chronic colitis in $TCR\alpha^{-/-}$ mice by infusion of free and toxin-conjugated anti-IL-7R mAb. Blockade of the IL-7R-dependent signaling pathway by anti-IL-7R mAb partially abrogated established colitis (our unpublished observation). Importantly, selective elimination of $IL\text{-}7R^{high}$ T cells by the administration of small amounts of saporin-conjugated anti-IL-7R mAb completely ameliorated ongoing colitis in $TCR\alpha^{-/-}$ mice. This saporin-conjugated anti-IL-7R mAb did not inhibit the in vitro proliferation of $CD4^+IL\text{-}7R^+$ spleen cells from normal mice, but did inhibit that of $IL\text{-}7R^{high}$ T cells from chronically inflamed mucosa of $TCR\alpha^{-/-}$ mice. This observation indicated that small amounts of saporin-conjugated anti-IL-7R mAb inhibited the proliferation or induced cell death of T cells expressing IL-7R at a high level that infiltrated in the chronic inflamed mucosa, but did not have an effect on cells expressing IL-7R at low or intermediate levels. This is explained by the fact that the amount of saporin binding to our anti-IL-7R mAb was extremely low. These results strongly confirmed that chronic inflammation in the colonic mucosa is mediated by the dysregulation of the mucosal IL-7/IL-7R signaling pathway. Treatment of wild-type mice with the same amount of saporin-conjugated anti-IL-7R mAb did not cause any change in the total cell number or a phenotypic change in spleen cells or LPLs. Depletion of $IL\text{-}7R^+$ or $CD4^+$ cells was not observed even after six treatments with 10 μg/body of saporin-conjugated anti-IL-7R mAb. Therefore, a therapy regulating LPLs expressing IL-7R at a high level is feasible in the treatment of chronic colitis without the deletion of cells expressing IL-7R at low or intermediate levels.

The mechanism by which the elimination of $IL\text{-}7R^{high}$ T cells leads to the amelioration of ongoing colitis should be defined. Our study showed that $IL\text{-}7R^{high}$ LPLs infiltrated in the lamina propria of colonic mucosa were activated and produced Th1- and Th2-type cytokines. Those activated $IL\text{-}7R^{high}$ mucosal T cells eventually produce inflammatory and proinflammatory cytokines that trigger a nonspecific inflammatory cascade. Therefore, it is not surprising that elimination of LPLs expressing IL-7R at a high level leads to the inhibition of ongoing colitis in chronic colitis mice.

Several clinical applications of IL-7 have been proposed, and many have been tested in mice (1, 22, 23). The major areas in which IL-7 appears to hold some clinical promise are antitumor activity, enhancement of lymphopoiesis, promotion of stem cell engraftment, and enhanced antimicrobial activity. However, only a few clinical applications have been conducted targeting IL-7R-bearing cells. Only a single trial was proposed for the therapy for hematologic malignancies by toxin-based destruction of IL-7R-bearing cells. Sweeney et al. (24) have constructed a recombinant fusion protein, DAB389 IL-7, composed of the catalytic and transmembrane domains of diphtheria toxin, fused to IL-7. They demonstrated that DAB389 IL-7 has a selective cytotoxic effect only on cells bearing the IL-7R, and that entry into target cells was mediated through the receptor. These results indicated that DAB389 IL-7 may be a novel reagent that possesses potential as a therapeutic agent against IL-7R-bearing cell-mediated disorders. They have also constructed an IL-2 version of the diphtheria toxin-based fusion toxin, DAB-IL-2, and applied this to the treatment of cutaneous T cell lymphoma (25). Preliminary studies using DAB-IL-2 for the treatment of severe rheumatoid arthritis and severe methotrexate-resistant psoriasis have also been reported (26, 27). Therefore, DAB389 IL-7 may be promising in the treatment of disorders other than hematological malignancies. All previous attempts were conducted to eliminate every IL-7R-bearing cell. The

present study was the first attempt to eliminate only T cells expressing IL-7R at a high level by toxin-based destruction of cells for the treatment of nonmalignant disorders, and we are currently investigating whether DAB389 IL-7 is effective in the treatment of chronic colitis.

This study provides a basis for practical application of therapy targeting T cells expressing IL-7R at a high level for the treatment of chronic intestinal inflammation in human inflammatory bowel disease. Human inflammatory bowel disease is thought to result from an inappropriate activation of the mucosal immune system driven by luminal flora (28). The activation of key immune cell populations is eventually accompanied by the production of a wide variety of nonspecific mediators of inflammation, including various other inflammatory and proinflammatory cytokines, chemokines, and growth factors. We suggest that T cells expressing IL-7R at a high level are one such key immune cell population. Therefore, therapeutic approaches targeting mucosal T cells expressing IL-7R at a high level may be feasible for the therapy of human inflammatory bowel disease.

Acknowledgments

We express special thanks to Prof. Hiroshi Kiyono and Dr. Masanobu Nanno for helpful discussion; Dr. Tatsuji Nomura and Kenichi Tamaoki for providing RAG-2$^{-/-}$ mice; Dr. Tetsuo Sudo for providing anti-IL-7R mAb; Drs. Yoshitaka Ueno, Yasushi Iwao, and Noriaki Watanabe for technical assistance; and Yuko Ito for manuscript preparation.

References

1. Fry, T. J., and C. L. Mackall. 2002. Interleukin-7: from bench to clinic. *Blood 99:3892.*
2. Watanabe, M., Y. Ueno, T. Yajima, Y. Iwao, M. Tsuchiya, H. Ishikawa, S. Aiso, T. Hibi, and H. Ishii. 1995. Interleukin 7 is produced by human intestinal epithelial cells and regulates the proliferation of intestinal mucosal lymphocytes. *J. Clin. Invest. 95:2945.*
3. Moore, T. A., U. von Freeden-Jeffry, R. Murray, and A. Zlotnik. 1996. Inhibition γδ T cell development and early thymocyte maturation in IL-7$^{-/-}$ mice. *J. Immunol. 157:2366.*
4. He, Y. W., and T. R. Malek. 1996. Interleukin-7 receptor α is essential for the development of γδ^{+} T cells, but not natural killer cells. *J. Exp. Med. 184:289.*
5. Maki, K., S. Sunaga, Y. Komagata, Y. Kodaira, A. Mabuchi, H. Karasuyama, K. Yokomura, J. I. Miyazaki, and K. Ikuta. 1996. Interleukin 7 receptor-deficient mice lack γδ T cells. *Proc. Natl. Acad. Sci. USA 93:7172.*
6. Adachi, S., H. Yoshida, K. Honda, K. Maki, K. Saijo, K. Ikuta, T. Saito, and SI. Nishikawa. 1998. Essential role of IL-7 receptor α in the formation of Peyer's patch analogue. *Int. Immunol. 10:1.*
7. Laky, K., L. Lefrancois, E. G. Lingenheld, H. Ishikawa, J. M. Lewis, S. Olson, K. Suzuki, R. E. Tigelaar, and I. Puddington. 2000. Enterocyte expression of interleukin 7 induces development of γδ T cells and Peyer's patches. *J. Exp. Med. 191:1569.*
8. Kanamori, Y., K. Ishimaru, M. Nanno, K. Maki, K. Ikuta, H. Nariuchi, and H. Ishikawa. 1996. Identification of novel lymphoid tissues in murine intestinal mucosa where clusters of c-kit^{+} IL-7R^{+} Thy-1^{+} lympho-hemopoietic progenitors develop. *J. Exp. Med. 184:1449.*
9. Suzuki, K., T. Oida, H. Hamada, O. Hitotsumatsu, M. Watanabe, T. Hibi, H. Yamamoto, E. Kubota, S. Kaminogawa, and H. Ishikawa. 2000. Gut cryptopatches: direct evidence of extrathymic anatomical sites for intestinal T lymphopoiesis. *Immunity 13:691.*
10. Watanabe, M., Y. Ueno, T. Yajima, S. Okamoto, T. Hayashi, M. Yamazaki, Y. Iwao, H. Ishii, S. Habu, M. Uehira, et al. 1998. Interleukin 7 transgenic mice development chronic colitis with decreased interleukin 7 protein accumulation in the colonic mucosa. *J. Exp. Med. 187:389.*
11. Watanabe, M., Y. Ueno, M. Yamazaki, and T. Hibi. 1999. Mucosal IL-7-mediated immune responses in chronic colitis-IL-7 transgenic mouse model. *Immunol. Res. 20:251.*
12. Okamoto, S., M. Watanabe, M. Yamazaki, T. Yajima, T. Hayashi, H. Ishii, M. Mukai, T. Yamada, N. Watanabe, B. A. Jameson, et al. 1999. A synthetic mimetic of CD4 is able to suppress disease in a rodent model of immune colitis. *Eur. J. Immunol. 29:355.*
13. Powrie, F., M. W. Leach, S. Mauze, L. B. Caddle, and R. L. Coffman. 1993. Phenotypically distinct subsets of CD4^{+} T cells induce or protect from chronic intestinal inflammation in C.B-17 scid. *Mice. Int. Immunol. 5:1461.*
14. Mombaerts, P., E. Mizoguchi, M. J. Grusby, L. H. Glimcher, A. K. Bhan, and S. Tonegawa. 1993. Spontaneous development of inflammatory bowel disease in T cell receptor mutant mice. *Cell 75:274.*
15. Mizoguchi, A., E. Mizoguchi, C. Chiba, G. M. Spiekerman, S. Tonegawa, C. Nagler-Anderson, and A. K. Bhan. 1996. Cytokine imbalance and autoantibody production in T cell receptor-α mutant mice with inflammatory bowel disease. *J. Exp. Med. 183:847.*
16. Takahashi, I., H. Kiyono, and S. Hamada. 1997. CD4^{+} T-cell population mediates development of inflammatory bowel disease in T-cell receptor α chain-deficient mice. *Gastroenterology 112:1876.*
17. Flavell, D. J. 1998. Saporin immunotoxins. *Curr. Top. Microbiol. Immunol. 234:57.*
18. Napolitano, L. A., R. M. Grant, S. G. Deeks, D. Schmidt, S. C. De Rosa, L. A. Herzenberg, B. G. Gerndiner, J. Andersson, and J. M. McCune. 2001. Increased production of IL-7 accompanies HIV-1-mediated T-cell depletion: implications for T-cell homeostasis. *Nat. Med. 7:73.*
19. Iijima, H., I. Takahashi, D. Kishi, J. K. Kim, S. Kawano, M. Hori, and H. Kiyono. 1999. Alteration of interleukin 4 production results in the inhibition of T helper type 2 cell-dominated inflammatory bowel disease in T cell receptor α chain-deficient mice. *J. Exp. Med. 190:607.*
20. Steidler, L., W. Hans, L. Schotte, S. Neirynck, F. Obermeiser, W. Falk, W. Fiers, and E. Remaut. 2000. Treatment of murine colitis by *Lactococcus lactis* secreting interleukin-10. *Science 289:1352.*
21. Mizoguchi, A., E. Mizoguchi, and A. K. Bhan. 1999. The critical role of interleukin 4 but not interferon γ in the pathogenesis of colitis in T-cell receptor α mutant mice. *Gastroenterology 116:320.*
22. Hofmeister, R., A. R. Khaled, N. Benbernou, E. Rajnavolgyi, K. Muegge, and S. K. Durum. 1999. Interleukin-7: physiological roles and mechanisms of action. *Cytokine Growth Factor Rev. 10:41.*
23. Appasamy, P. M. 1999. Biological and clinical implications of interleukin-7 and lymphopoiesis. *Cytokines Cell. Mol. Ther. 5:25.*
24. Sweeney, E. B., F. M. Foss, J. R. Murphy, and J. C. vaderSpek. 1998. Interleukin 7 (IL-7) receptor-specific cell killing by DAB389IL-7: a novel agent for the elimination of IL-7 receptor positive cells. *Bioconjug. Chem. 9:201.*
25. Duvic, M., J. Cather, J. Maize, and A. E. Frankel. 1998. DAB389IL2 diphtheria fusion toxin products clinical responses in tumor stage cutaneous T cell lymphoma. *Am. J. Hematol. 58:87.*
26. Gottlieb, S. L., P. Gilleaudeau, R. Johnson, L. Estes, T. G. Woodworth, A. B. Gottlieb, and J. G. Krueger. 1995. Response of psoriasis to a lymphocyte-selective toxin (DAB389IL-2) suggests a primary immune, but not keratinocyte, pathogenic basis. *Nat. Med. 1:442.*
27. Bagel, J., W. T. Garland, D. Breneman, M. Holick, T. W. Littlejohn, D. Crosby, H. Faust, D. Fivenson, and J. Nichols. 1998. Administration of DAB389IL-2 to patients with recalcitrant psoriasis: a double-blind, phase II multicenter trial. *J. Am. Acad. Dermatol. 38:938.*
28. Podolsky, D. K. 2002. Inflammatory bowel disease. *N. Engl. J. Med. 347:417.*

MOLECULAR AND CELLULAR BIOLOGY, July 2004, p. 6298–6310 Vol. 24, No. 14
0270-7306/04/$08.00+0 DOI: 10.1128/MCB.24.14.6298–6310.2004

Interferon Regulatory Factor 1 (IRF-1) and IRF-2 Distinctively Up-Regulate Gene Expression and Production of Interleukin-7 in Human Intestinal Epithelial Cells

Shigeru Oshima,[1]† Tetsuya Nakamura,[1]† Shin Namiki,[1] Eriko Okada,[1] Kiichiro Tsuchiya,[1] Ryuichi Okamoto,[1] Motomi Yamazaki,[1] Takanori Yokota,[2] Masatoshi Aida,[3] Yuki Yamaguchi,[3] Takanori Kanai,[1] Hiroshi Handa,[3] and Mamoru Watanabe[1]*

Department of Gastroenterology and Hepatology[1] and Department of Neurology and Neurological Sciences,[2] Graduate School, Tokyo Medical and Dental University, Bunkyo-ku, Tokyo 113-8519, and Graduate School of Bioscience and Biotechnology, Tokyo Institute of Technology, Yokohama 226-8501,[3] Japan

Received 10 September 2003/Returned for modification 16 January 2004/Accepted 19 April 2004

Intestinal epithelial cell-derived interleukin (IL)-7 functions as a pleiotropic and nonredundant cytokine in the human intestinal mucosa; however, the molecular basis of its production has remained totally unknown. We here showed that human intestinal epithelial cells both constitutively and when induced by gamma interferon (IFN-γ) produced IL-7, while several other factors we tested had no effect. Transcriptional regulation via an IFN regulatory factor element (IRF-E) on the 5′ flanking region, which lacks canonical core promoter sequences, was pivotal for both modes of IL-7 expression. IRF-1 and IRF-2, the latter of which is generally known as a transcriptional repressor, were shown to interact with IRF-E and transactivate IL-7 gene expression in an IFN-γ-inducible and constitutive manner, respectively. Indeed, tetracycline-inducible expression experiments revealed that both of these IRF proteins up-regulated IL-7 protein production, and their exclusive roles were further confirmed by small interfering RNA-mediated gene silencing systems. Moreover, these IRFs displayed distinct properties concerning the profile of IL-7 transcripts upon activation and expression patterns within human colonic epithelial tissues. These results suggest that the functional interplay between IRF-1 and IRF-2 serves as an elaborate and cooperative mechanism for timely as well as continuous regulation of IL-7 production that is essential for local immune regulation within human intestinal mucosa.

Intestinal epithelial cells (IECs) function as active participants in local immune regulation via the secretion of a variety of cytokines. Among these, interleukin-7 (IL-7) is particularly important in terms of its pleiotropic functions in the intestinal immune system. Studies have demonstrated that IEC-derived IL-7 stimulates the proliferation of lamina propria lymphocytes and intraepithelial lymphocytes (IELs) (5, 30) and also enhances cytokine release from lamina propria lymphocytes in humans (20). In addition, analyses in mice have revealed the nonredundant functions of IL-7, because inactivation of IL-7 or the IL-7 receptor gene resulted in severely impaired development of γδ-IELs, Peyer's patches, and cryptopatches, all of which play critical roles in mucosal immune regulation (13, 21, 29). These findings suggest that IL-7 production from IECs might be tightly controlled for variable levels of production that properly respond to the altered status of mucosal lymphocytes and also for the constitutive levels of secretion that might support the nonredundant functions of IL-7, for example, on the development of gut-associated lymphoid tissues. Previously, our group has demonstrated that the mRNA and protein of IL-7 are expressed throughout the epithelial layer of human colonic tissues, and the epithelial goblet cells are the type of cells where the expression of IL-7 is relatively abundant (30). To date, however, the mechanisms of IL-7 production in human IECs are poorly defined.

Lack of knowledge about the mechanism of IL-7 production is not confined to IECs but is also the case with other tissue-derived cells of human origin. Previous reports demonstrated that IL-7 production from human bone marrow (BM) stromal cells, the major cell type from which IL-7 is produced in vivo, was regulated by several cytokines such as IL-1, tumor necrosis factor alpha (TNF-α) and transforming growth factor beta (TGF-β) (27, 34); however, the intracellular mechanisms of these regulations have remained unclear. In addition, little is known about the mechanisms by which IL-7 is constitutively produced, while such cells as BM stromal cells exhibited the ability to produce a substantial amount of IL-7 even in the absence of specific cytokines in vitro (27, 34). Moreover, studies on murine tissue-derived cells rather complicated the question as to the mechanisms of IL-7 production in human cells, since these studies implied a different mechanism for murine IL-7 gene expression (3), despite a high degree of conservation in the 5′ flanking region of the IL-7 genes of both species (3, 8, 23). For example, in murine keratinocytes Pam 212 cells, ex-

* Corresponding author. Mailing address: Department of Gastroenterology and Hepatology, Graduate School, Tokyo Medical and Dental University, 1-5-45 Yushima, Bunkyo-ku, Tokyo 113-8519, Japan. Phone: 81 3 5803 5973. Fax: 81 3 5803 0262. E-mail: mamoru.gast@tmd.ac.jp.

† S.O. and T.N. contributed equally to this work.

pression of the IL-7 gene was not influenced by IL-1, TNF-α, or TGF-β but was up-regulated by another cytokine, gamma interferon (IFN-γ) (3), indicating that murine cells respond differently than human BM stromal cells to these cytokines (27, 34). These collective findings suggest that IL-7 production might be under the control of a tissue-specific and/or a species-specific regulatory mechanism. Therefore, it seems crucial to clarify the mechanisms of IL-7 production in human IECs to gain a better understanding of the functions of this cytokine on local immune regulation.

In this study, using human colonic epithelial cell lines, we showed that IL-7 protein was produced both constitutively and in response to IFN-γ in human IECs. The transcriptional regulation via an interferon regulatory factor element (IRF-E) was important for IL-7 production in human IECs, which is consistent with the previous report on murine keratinocytes. Of note, it was found that not only IRF-1 but also IRF-2, generally known as a transcriptional repressor, up-regulated IL-7 production. Intriguingly, IRF-1 and IRF-2 exclusively exerted their functions in an IFN-γ-inducible and constitutive manner, respectively, with properties to induce different sets of IL-7 transcript upon activation. Along with the demonstration that both IRF-1 and IRF-2 were expressed in normal human colonic epithelial cells, these data suggest that the functional interplay between IRF-1 and IRF-2 might serve as an elaborate mechanism for the finely tuned regulation of IL-7 production that is indispensable for local immune regulation within the human intestinal mucosa.

MATERIALS AND METHODS

Cell culture. Human colon carcinoma-derived DLD-1 and HT29-18N2 cells were maintained in Dulbecco's modified Eagle medium supplemented with 10% fetal bovine serum and 1% penicillin-streptomycin. Except where indicated otherwise, cells were seeded at a density of 3×10^5 cells/ml in the medium 36 h prior to each experiment.

ELISA. Cells at a density of 8×10^5 cells per ml of culture medium were seeded onto 24-well plates. After 36 h of culture, the medium was removed, and the cells were washed twice with phosphate-buffered saline. Following the addition of 1 ml of culture medium alone, or medium containing either human IL-1β, TNF-α, TGF-β, IFN-γ (PeproTec), or doxycycline (DOX; Clontech), cells were cultured for 24 h, and human IL-7 protein levels in the culture supernatants were measured by a human IL-7 enzyme-linked immunosorbent assay (ELISA) kit (R&D Systems).

Semiquantitative reverse transcription (RT)-PCR. Total RNA was isolated by using Trizol reagent (Invitrogen) according to the manufacturer's instructions. Aliquots of 5 μg of total RNA were used for cDNA synthesis in 21 μl of reaction volume. One microliter of cDNA was amplified with 0.25 U of LA *Taq* polymerase (TaKaRa) in a 25-μl reaction. Sense (S) and antisense (AS) primers used here were as follows: S1, 5′-AGCTTGCTCCTGCTCCAGTT-3′; S2, 5′-GAGA TCATCTGGGAAGTCTTTTACC-3′; S3, 5′-ACTTGTGGCTTCCGTGCACA CATTA-3′; AS1, 5′-TGCATTTCTCAAATGCCCTAATCCG-3′; and AS2, 5′-ATCCGCCAGCAGTGTACTTTCAGTT-3′ for human IL-7 (see Fig. 2A). For glyceraldehyde 3-phosphate dehydrogenase (G3PDH) amplification, the primers were5′-TGAAGGTCGGAGTCAACGGATTTGGT-3′ (S) and and 5′-CATGT GGGCCATGAGGTCCACCAC-3′ (AS). Each cycle of PCR amplification consisted of denaturation at 94°C for 30 sec, annealing at 61°C for 30 sec, and extension at 72°C for 30 sec. Twenty-seven cycles were performed for IL-7, and 17 cycles were performed for G3PDH, and the amplification for each gene was in the linear curve under these conditions. PCR products were separated on 1.5% agarose gels, stained by ethidium bromide, and visualized by using a Lumi-Imager F1 system (Roche).

Northern blotting. Poly(A)$^+$ mRNA was isolated by using a FastTrack 2.0 kit (Invitrogen) according to the manufacturer's instructions. Northern blotting was performed as described previously (22) by using 15 μg of poly(A)$^+$ mRNA. The cDNA probe corresponding to nucleotides at positions −55 to +681 (coding sequence [CS] probe) and −539 to −242 (5′ untranslated region [UTR] probe) for human IL-7 were generated by RT-PCR by using the primers S1/AS1 and S3/AS2, respectively, from an RNA sample of DLD-1 cells as described above. The probe for G3PDH was also generated by RT-PCR by using the primers described above. Hybridization was carried out at 42°C overnight for IL-7 and at 55°C for 2 h for G3PDH.

RLM-RACE. Determination of the transcription initiation sites of the human IL-7 gene was accomplished by RNA ligase-mediated [RLM] 5′ rapid amplification of cDNA ends [RACE] by using a GeneRacer Kit (Invitrogen). In brief, poly(A)$^+$ mRNAs extracted from IFN-γ-stimulated (6 h) DLD-1 cells were treated with calf intestinal phosphatase to eliminate 5′ phosphates from truncated mRNA without affecting 5′ capped intact mRNA. The dephosphorylated RNA was then treated with tobacco acid pyrophosphatases to remove the 5′ cap structure. The GeneRacer RNA Oligo was ligated to the 5′ end of the decapped mRNA by using T4 RNA ligase. First-strand cDNA synthesis was performed by reverse-transcribing the ligated mRNA in the presence of the GeneRacer oligo dT primer. Sequential PCRs were performed by using a primer set of the GeneRacer 5′ primer and 3′ reverse IL-7 gene-specific primer 1 (GSP-1) and then by using the nested primer set of the GeneRacer 5′ nested primer and 3′ reverse IL-7 GSP-2 to amplify only the cDNAs that have the GeneRacer RNA Oligo ligated to the 5′ end. As a control, PCR with a primer set for amplifying the 5′ part of the human β-actin gene was also performed in parallel, according to the manufacturer's recommendation. The primers used were 5′-TGCCCTA ATCCGTTTTGACCATGGTG-3′ (IL-7 GSP-1) and 5′-GCAACAGAACAAG GATCAGGGGAGG-3′ (IL-7 GSP-2). PCR products of around 600 and 300 bp were gel purified and cloned into the pGEM-T vector (Promega) independently, and then 10 clones of each were sequenced. All the clones contained the IL-7 gene sequence along with the adapter sequences, indicating these clones to be derived from mRNAs retaining complete 5′ ends.

Plasmids. The human IL-7 DNA fragment between either position −3194, −1322, −609, or −282 and −3 was amplified from human genomic DNA by PCR and ligated into the pGL3 Basic luciferase reporter plasmid (Promega) to create −3194-Luc, −1322-Luc, −609-Luc, and −282-Luc. The nucleotide position number was assigned relative to the translation start site (+1). A series of 5′ deletions of the −609-Luc, shown as −362-Luc, −251-Luc, and −215-Luc, was constructed by unidirectional digestion by using an exonuclease III. An internal deletion mutant −609-Luc-Δ-282/-251 was constructed by PCR-mediated mutagenesis. Plasmids −609-mtIRF-E-Luc and −282-mtIRF-E-Luc, both of which contain a 4-bp mutation within IRF-E, were also constructed by PCR-mediated mutagenesis. Introduced mutations and the wild-type sequences within the region of positions −280 to −253 were given with top strand sequences as follows: mutant, 5′-AAGCGCAAAGTAGAGGCTGAGGGTACAC-3′ (underlined residues indicate introduced mutations); wild type, 5′-AAGCGCAAAGTAGAAA CTGAAAGTACAC-3′. Expression vectors pcDNA3-IRF-1 and pcDNA3-IRF-2 were prepared by subcloning the PCR-amplified open reading frame of human IRF-1 and IRF-2 cDNA into a pcDNA3 (Invitrogen). To construct tetracycline (TET)-inducible expression plasmids, the open reading frames of IRF-1 and IRF-2 were subcloned into a pcDNA4/TO/Myc/His (Invitrogen) in frame. All constructs were verified by DNA sequencing.

Transient transfection and reporter assays. DLD-1 cells seeded in a 60-mm culture dish were transfected with 3 μg of reporter plasmid along with 10 ng of pRL-tk plasmid (Promega) as described previously (22). Cells were harvested 24 h after transfection, lysed by three cycles of freezing and thawing, and then luciferase activities were measured by a luminometer (Turner Designs). Luciferase activities as indicated by arbitrary unit were normalized by renilla luciferase activities in each sample.

EMSA. The preparation of nuclear extracts and electrophoretic mobility shift assays (EMSA) were performed essentially as described previously (22), except for the use of 0.5 μg of poly(dI-dC) · poly(dI-dC) per binding reaction. A DNA probe and its mutated version were prepared by annealing oligonucleotides as follows: top strand, 5′-AAGCGCAAAGTAGAAACTGAAAGT-3′, and bottom strand, 5′-GTGTACTTTCAGTTTCTACTTTG-3′, for the wild-type probe; and top strand, 5′-AAGCGCAAAGTAGAGGCTGAGGGT-3′, bottom strand, 5′-GTGTACCCTCAGCCTCTACTTTG-3′, for the mutant probe. For competition experiments, a 20-fold excess of unlabeled double-stranded probe or its mutated version was added prior to the labeled probe. In supershift experiments, antibodies (Santa Cruz Biotechnology) against either IRF-1 (catalogue no. sc-497), IRF-2 (sc-498), IRF-3 (sc-9082), IRF-4 (sc-6059), IRF-7 (sc-9083), IRF-8 (sc-6058), or IRF-9 (sc-496) were used.

Immunoblotting. Immunoblotting was performed as described elsewhere (22). Twenty-five micrograms of nuclear extracts was analyzed by using anti-IRF-1 (catalogue no. sc-497), anti-IRF-2 (sc-498), and anti-upstream factor (USF)-2 (sc-861) antibodies (all from Santa Cruz Biotechnology) at a 1:500 dilution as a

primary antibody. Proteins were visualized with an enhanced chemiluminescence detection system (Amersham Bioscience).

Establishing tetracycline-regulated IRF-1- and IRF-2-expressing DLD-1 cell lines. Sublines of DLD-1 cells, in which the expression of either IRF-1 or IRF-2 is inducible under the control of the addition of TET, were established by using a T-REx System (Invitrogen). In brief, a DLD-1-derived subclone that constitutively expresses the TET repressor (TR) was created by transfecting parental DLD-1 cells with a plasmid pcDNA6/TR (Invitrogen). Several clones were selected in the culture medium containing blasticidin (7.5 μg/ml; Invitrogen). An appropriate clone was isolated, designated as DLD-1/TR cells, and then transfected with either expression plasmid pcDNA4/TO/IRF-1-Myc/His or pcDNA4/TO/IRF-2-Myc/His. Cells stably expressing each of these genes were selected in the presence of 750 μg of Zeocin (Invitrogen) per ml to establish the sublines designated as DLD-1/TR/IRF-1-tag or DLD-1/TR/IRF-2-tag cells. In all experiments, we used DOX as an alternative inducer of gene expression because it has a longer half-life than TET.

siRNA experiments. All small interfering RNA (siRNA) duplex oligonucleotides were synthesized and subsequently annealed for use. DLD-1 cells were seeded at a density of 3×10^5 cells per ml onto a 24-well plate or a 100-mm culture dish. After 36 h, cells were transfected with 100 nM siRNA oligonucleotides as described previously (37), and the siRNA-containing medium was removed after 12 h of transfection. Cells were cultured for an additional 12 h under the usual conditions, and then the medium was exchanged with either the medium alone or medium containing IFN-γ. For immunoblotting analysis, cells were collected from the 100-mm dishes after 12 h of medium exchange, and the nuclear extracts were isolated. For the ELISA, the culture supernatants were collected from the 24-well plates after 24 h of medium exchange. The sequences of siRNAs used here were as follows (S strand only): IRF-1, CCAAGAACCA GAGAAAAGA*TT*; IRF-2, CUCUUUAGAAACUGGGCAA*TT*; and negative control (G85R mutant superoxide dismutase), UGUUGGAGACUUCGGCAA U*TT*. Italicized letters indicate deoxynucleotides.

ChIP assays. A chromatin immunoprecipitation (ChIP) assay was performed essentially as described previously (24) with some modifications. DLD-1 cells seeded onto a 150-mm dish were stimulated with IFN-γ or left untreated for 6 h, cross-linked with 1% formaldehyde for 5 min at room temperature, and then quenched by adding glycine. Cells were washed with phosphate-buffered saline, resuspended in 1 ml of lysis buffer (10 mM Tris-HCl [pH 8.0], 0.25% Triton X-100, 10 mM EDTA, and 0.5 mM EGTA) and left on ice for 10 min. After centrifugation, the nuclei were washed with 1 ml of wash buffer (10 mM Tris-HCl [pH 8.0], 200 mM NaCl, 10 mM EDTA, and 0.5 mM EGTA, 10 mM sodium butyrate, 20 mM β-glycerophosphate, 100 μM sodium orthovanadate, 1 μM microcystin, and the protease inhibitor cocktail) and resuspended in 400 μl of sonication buffer (10 mM Tris-HCl [pH 8.0], 100 mM NaCl, 1 mM EDTA, and 0.5 mM EGTA). The sonication was performed in two steps by using a VP-152 system (TAITEC); the first step was carried out for 5 min, followed by the addition of 50 μl of 10% sodium dodecyl sulfate (SDS) and incubation for 1 h to solubilize the chromatin, and then the second sonication was performed for 4 min. This yielded genomic fragments with an average size of 500 bp. Aliquots (100-μl) of sheared chromatin were diluted into 1 ml of radioimmunoprecipitation assay (RIPA) buffer (10 mM Tris-HCl [pH 8.0], 1% Triton X-100, 0.1% SDS, 0.1% sodium deoxycholate, 1 mM EDTA, 0.5 mM EGTA, and 140 mM NaCl) and precleared with 50 μl of protein G-Sepharose (50% slurry in RIPA buffer) for 1 h at 4°C. Immunoprecipitation was performed overnight at 4°C with 10 μg of an anti-IRF-1 (catalogue no. sc-497), anti-IRF-2 (sc-498), normal mouse immunoglobulin G (IgG; sc-2025) (all from Santa Cruz Biotechnology), or an antihistone H3 antibody (Abcam, Inc.). A 20-μl aliquot of 50% protein G-Sepharose slurry (same as above but containing 2 mg of herring sperm DNA per ml and 2 mg of bovine serum albumin per ml) was added to each and incubated for 1 h at 4°C. Precipitates were washed sequentially in RIPA buffer three times, in 0.5 M NaCl RIPA buffer (same as RIPA buffer but with 500 mM NaCl) three times, in LiCl wash buffer (10 mM Tris-HCl [pH 8.0], 0.25 M LiCl, 1% NP-40, 1% sodium deoxycholate, 1 mM EDTA, 1 mM EGTA, 10 mM sodium butyrate, 100 μM sodium orthovanadate, and the protease inhibitor cocktail) twice, and in TE buffer (10 mM Tris-HCl [pH 8.0], 1 mM EDTA) twice, for 3 min for each wash. Samples were extracted twice with 50 μl of elution buffer (1% SDS, 0.1 M NaHCO3, 10 mM dithiothreitol) and digested with 2 μg of proteinase K at 37°C for 4 h. Then 4 μl of 5 M NaCl was added, and the samples were incubated at 65°C overnight to reverse cross-linking. DNA fragments were recovered by phenol-chloroform extraction and ethanol precipitation.

The genomic DNA fragments in the immunoprecipitated samples were analyzed by PCR by using a primer set for amplifying the −539 to −159 region of the human IL-7 gene (5′-ACTTGTGGCTTCCGTGCACACATTA-3′ and 5′-GACTGCAGTTTCATCCATCCCAAG-3′) to detect the IRF-E-containing fragment, and another set for the +976 to +1337 region (5′-GCTCTTTCTTTT GATGGCTACTCCG-3′ and 5′-TAGCCCATGATTCATATAACTGTGC-3′; numbers indicate the positions on the genomic DNA relative to the translation start site) (see Fig. 8A) as controls. Initially, quantitative PCR on a LightCycler system (Roche) was performed to quantify the immunoprecipitated DNA. A 5-μl aliquot from a total of 100 μl of DNA solution was amplified and the threshold cycle was obtained from each amplification curve. In practice, DNA fragments were nonspecifically and reproducibly recovered after the ChIP assay in the absence of specific antibody but were usually amplified 5 to 6 cycles later than specifically recovered fragments. By using software provided by the manufacturer, the amount of DNA fragment in each sample was calculated relative to the standard curve obtained by the three different dilutions of input DNAs (10, 1, and 0.1%). Three independent chromatin preparations were made, and the average value obtained for each sample was indicated as a percentage of total input DNA. The same amounts of DNA samples or the diluted inputs were also analyzed by conventional PCR in parallel with the following parameters: denaturation at 94°C for 15 s, annealing at 61°C for 30 s, and extension at 72°C for 30 s for 37 cycles. The products were resolved by agarose gel electrophoresis, stained with ethidium bromide, and visualized by using a Lumi-Imager F1 system (Roche).

Immunohistochemistry. Normal colonic mucosae were obtained from three patients with colorectal cancer who underwent colectomy. Written informed consent was obtained from all patients, and these experiments were approved by the Tokyo Medical and Dental University Hospital Committee on Human Subjects. Samples fixed by 4% paraformaldehyde were cut into 8 μm-thick sections, treated with 0.5% hydrogen peroxide in methanol solution, blocked for 45 min, and then incubated with either an anti-IRF-1 (catalogue no. sc-497; Santa Cruz Biotechnology), an anti-IRF-2 (sc-13042), or purified rabbit IgG (10 mg/ml; negative control) overnight at 4°C. The sections were incubated with biotinylated goat antirabbit IgG for 60 min and reacted with streptavidin-enzyme conjugates (Vector Laboratories Inc), and then the peroxidase activities were developed by diaminobenzidin. After the samples were counterstained with hematoxylin, the localization of IRF-1 or IRF-2 was examined by light microscopy.

RESULTS

Human IECs constitutively produce IL-7, and IL-1, TNF-α, and TGF-β have no influence on the levels of IL-7 production, but IFN-γ does. To investigate the mechanisms of IL-7 production in human IECs, human colonic epithelial cell lines, DLD-1 and HT29-18N2 cells, were analyzed. Previous reports showed that both IL-1 and TNF-α had enhancing effects on IL-7 production in human BM stromal cells or osteoblasts (34), while TGF-β had suppressive effects on IL-7 production in BM stromal cells (27). In contrast, shown with murine keratinocytes, none of these cytokines had any effect, while IFN-γ solely exhibited enhancing effects on IL-7 mRNA expression among various factors (3). Therefore, to test whether IL-7 production in human IECs is also diversely regulated by these cytokines, DLD-1 and HT29-18N2 cells were incubated for 24 h with either IL-1, TNF-α, TGF-β, IFN-γ, or the medium alone, and IL-7 production was measured by ELISA. As shown in Fig. 1, both of these cells constitutively produced substantial amounts of IL-7 protein, with a higher concentration per cell number in DLD-1 than in HT29-18N2 cells. In addition, treatment with IFN-γ significantly enhanced IL-7 production in both cell types, while stimulation with IL-1, TNF-α, or TGF-β had no effect (Fig. 1). We also tested the possibility that TGF-β might act as an inhibitory factor not for the constitutive but for the inducible production of IL-7, but treatment with TGF-β did not affect IFN-γ-inducible IL-7 production (Fig. 1). These data indicated that human IECs produce IL-7 both constitutively and in response to IFN-γ, while several other cytokines have no regulatory effect on this process.

Transcription start sites of the human IL-7 gene are clustered within two distinct regions, and IFN-γ preferentially